

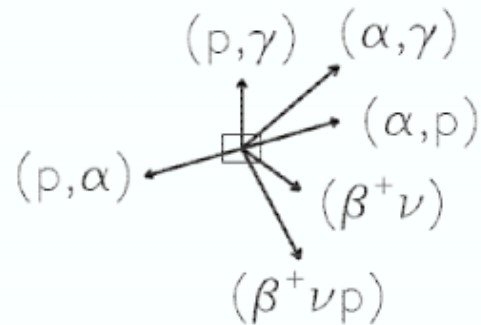
**From nuclear physics experiments
to reaction rates in stars**

Outline

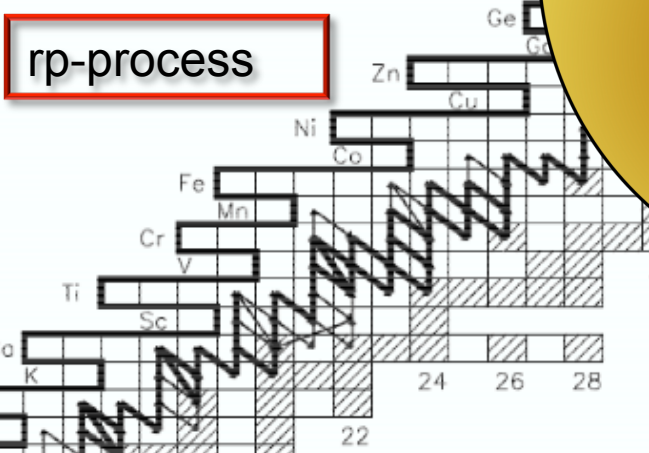
1. Introduction
2. **Astrophysics** - Nucleosynthesis processes (briefly)
3. **Nuclear Physics** – Reaction rate and resonant reactions
4. **Experimental techniques**
 - i. Terminology
 - ii. Direct vs indirect
 - iii. Schematic of experiment
5. **Direct measurements**
6. **(Indirect techniques – if time)**

2. Nucleosynthesis processes

Heavy element nucleosynthesis and neutron capture reactions – Rene's lecture



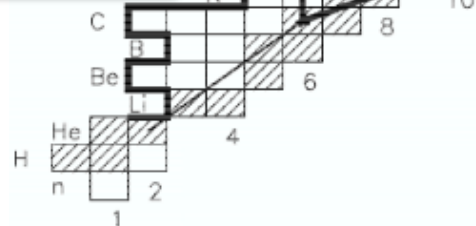
rp-process



αp -process

NeNa, MgAl cycles

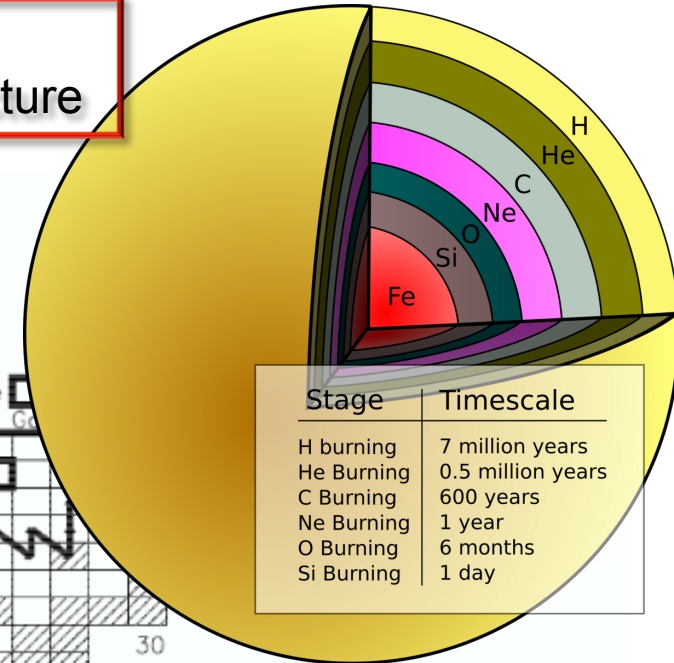
(H)CNO cycles



Non-explosive burning – Falk and Raphael's lectures

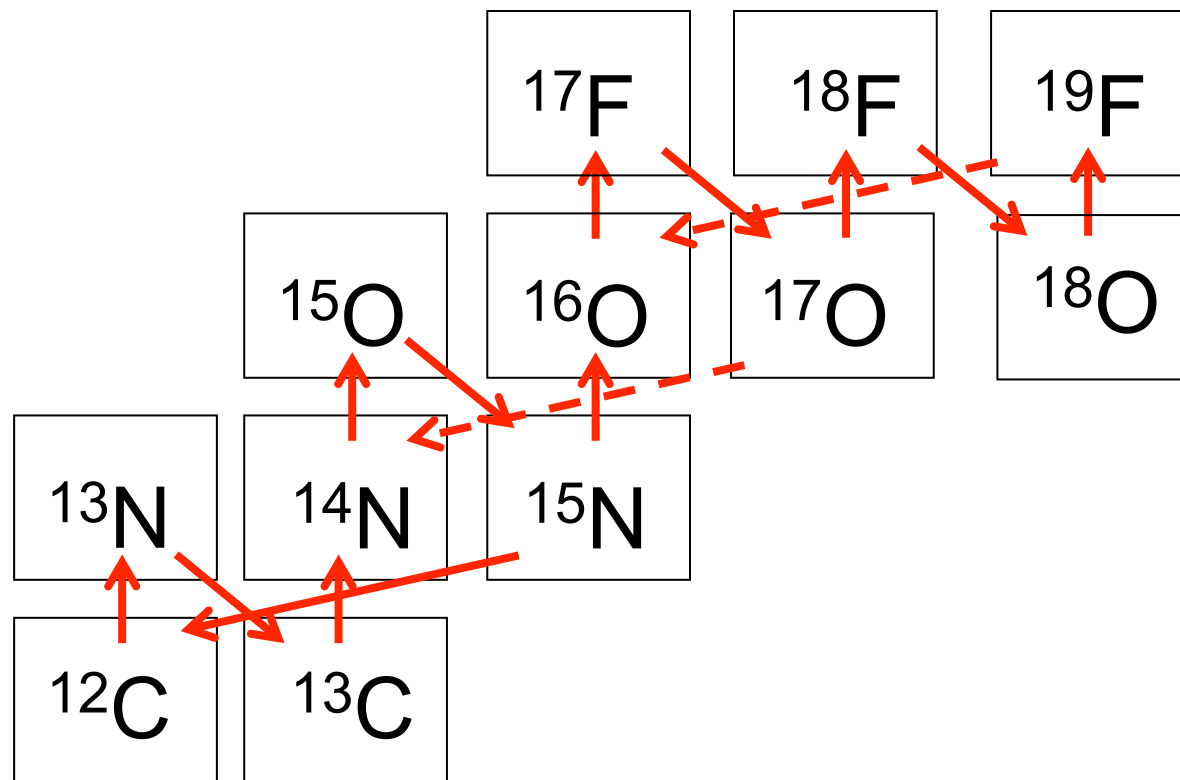
Explosive burning – Chris's lecture

Fig 3.6 from Iliadis – Nuclear Physics of Stars



T=0.5 GK

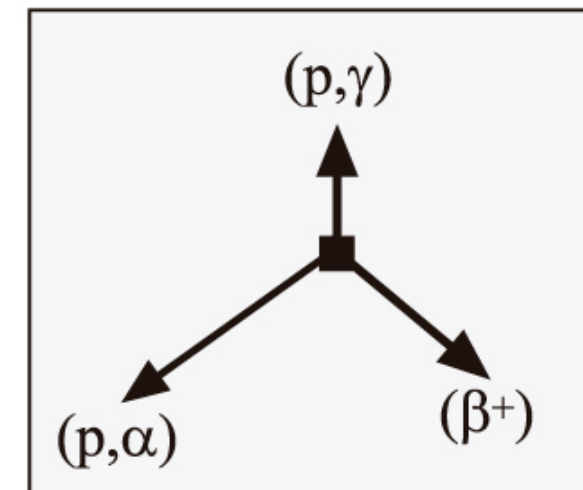
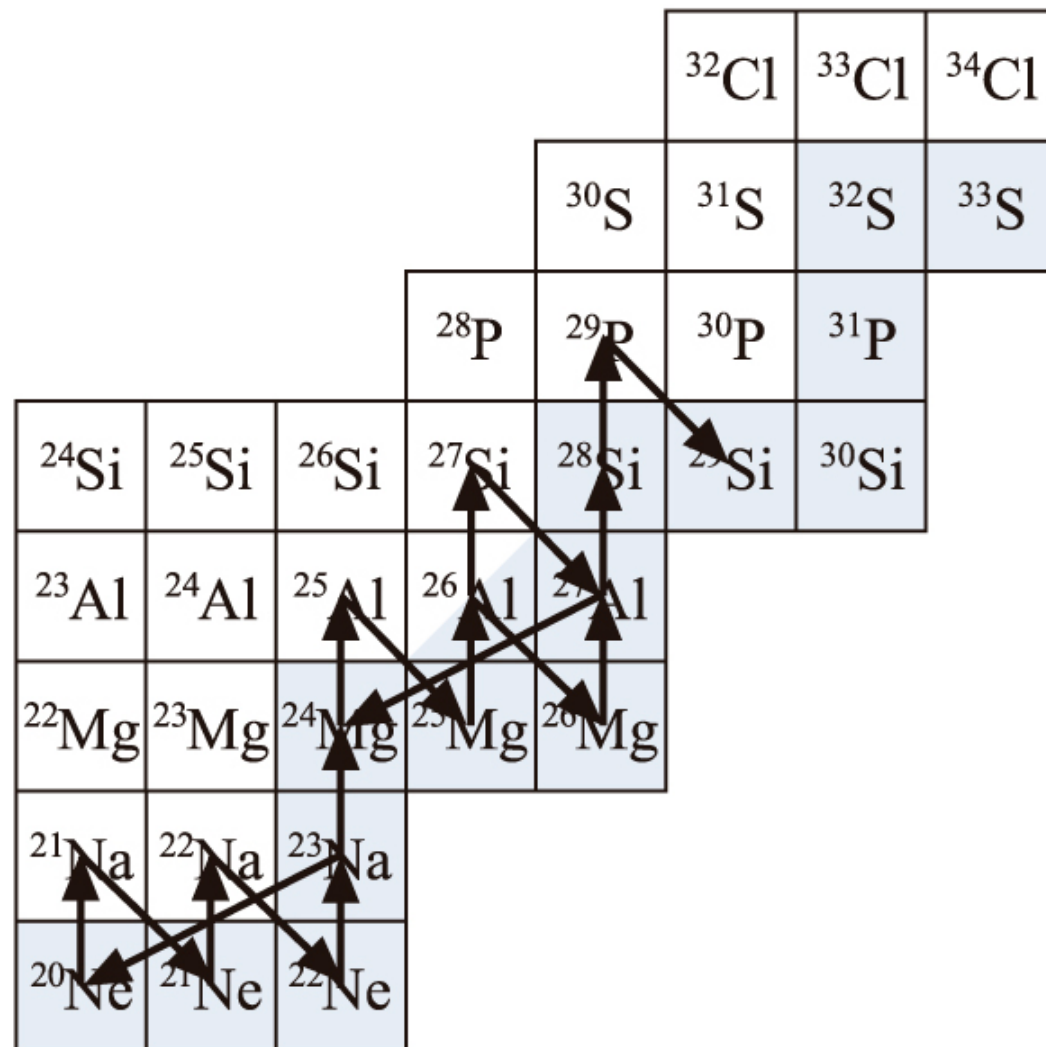
Hydrogen burning – CNO cycles – energy generation



The CNO material is conserved in these reactions – it simply acts as a catalyst to burn $4\text{p} \rightarrow ^4\text{He}$

Side branches occur at points where two reactions compete [(p, γ) vs (p, α)].
Need to know both cross sections to determine how much flux goes round each branch

Hydrogen burning beyond CNO mass region – nucleosynthesis



From Jose.

Reaction types and energies

- ✧ (p, γ)
- ✧ (α , γ)
- ✧ (p, α)
- ✧ (α ,p)
- ✧ (α ,n)
- ✧ *plus a few heavier reactions (e.g. $^{12}C+^{12}C$, ...)*

Typical centre of mass energies: 0.1 - 5 MeV.

Need to know temperature of astrophysics site – Gamow window.

Often competition between channels (e.g. (p, γ) vs (p, α)) is more important than actual rates.

3. Nuclear reaction rates

Nuclear reaction rates

Key input to stellar models is the astrophysical reaction rate.

$$\langle \sigma v \rangle = \left(\frac{8}{\pi\mu}\right)^{(1/2)} \frac{1}{(kT)^{3/2}} \int_0^\infty E \sigma(E) e^{-E/kT} dE$$

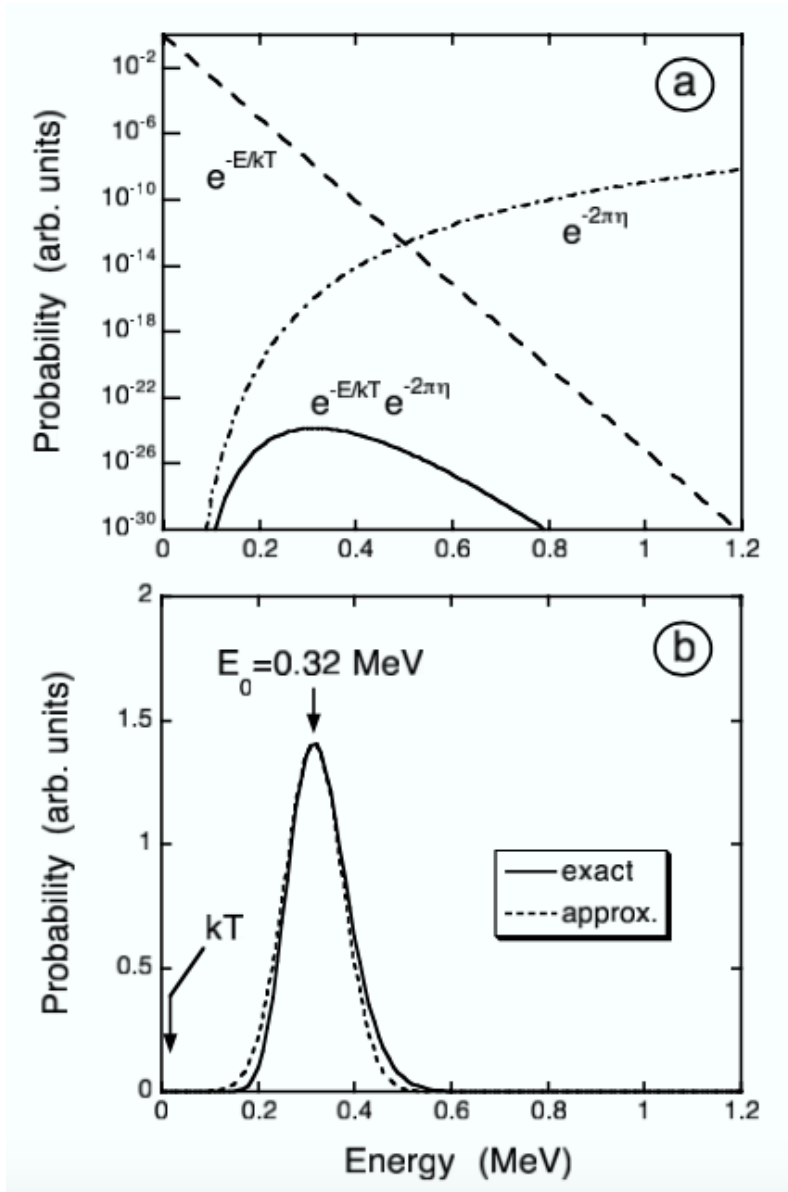
So need to know the cross section as a function of energy.

In this lecture we will cover the case for light nuclei, where the nuclear level density is low and the structure and location of individual states plays an important role.

=> resonant reaction rates

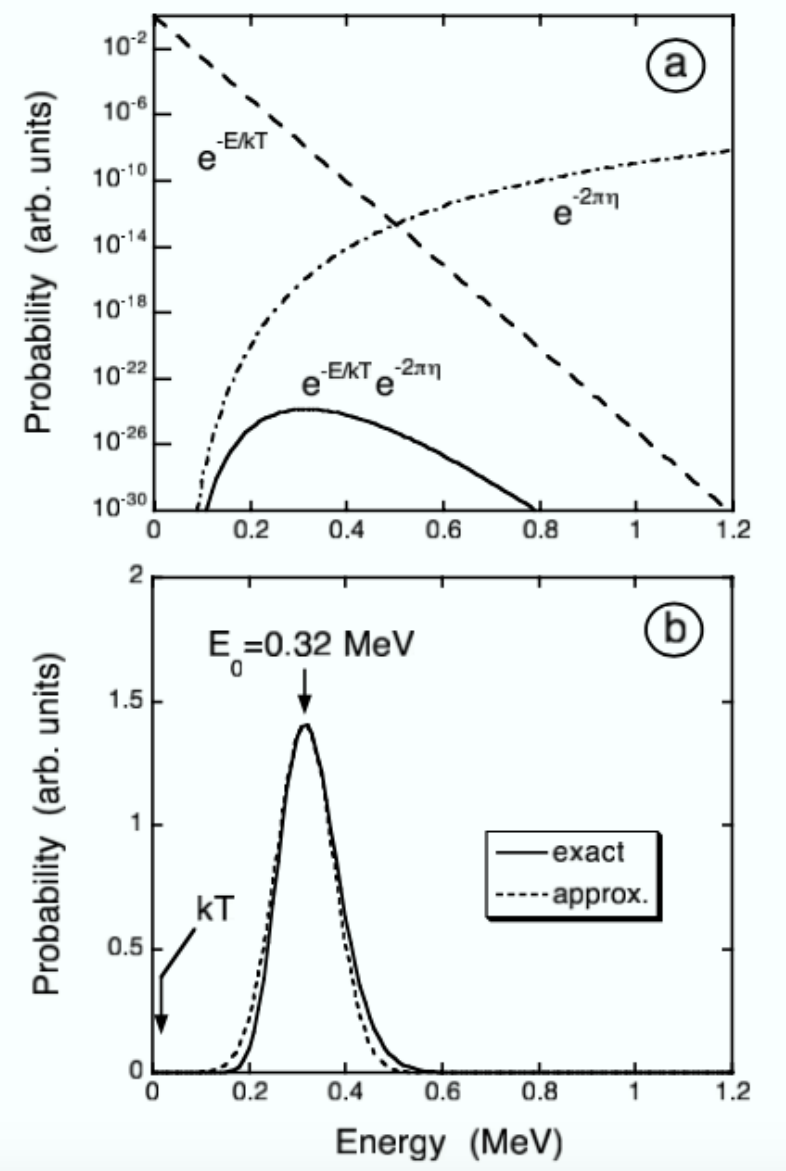
First we need to define the relevant energy range over which we need to know the cross section – the Gamow window.

Gamow window



From Iliadis.

Gamow window



$$E_G = 0.122(z_0^2 z_1^2 \mu T_9^2)^{1/3}$$
$$\Delta_G = 0.2368(z_0^2 z_1^2 \mu T_9^5)^{1/6}$$

As the charge of the projectile and target increase, the Gamow peak becomes broader.
However, the area under the peak drops quickly.

Therefore the total reaction rate, which is proportional to the area under the peak, also drops significantly.

For a given temperature, the **nuclear reactions with the smallest Coulomb barriers dominate**.

From Iliadis.

Astrophysical S-factor

It is also useful to introduce the Astrophysical S-factor:

$$\sigma = S(E) \frac{1}{E} e^{-2\pi\eta}$$

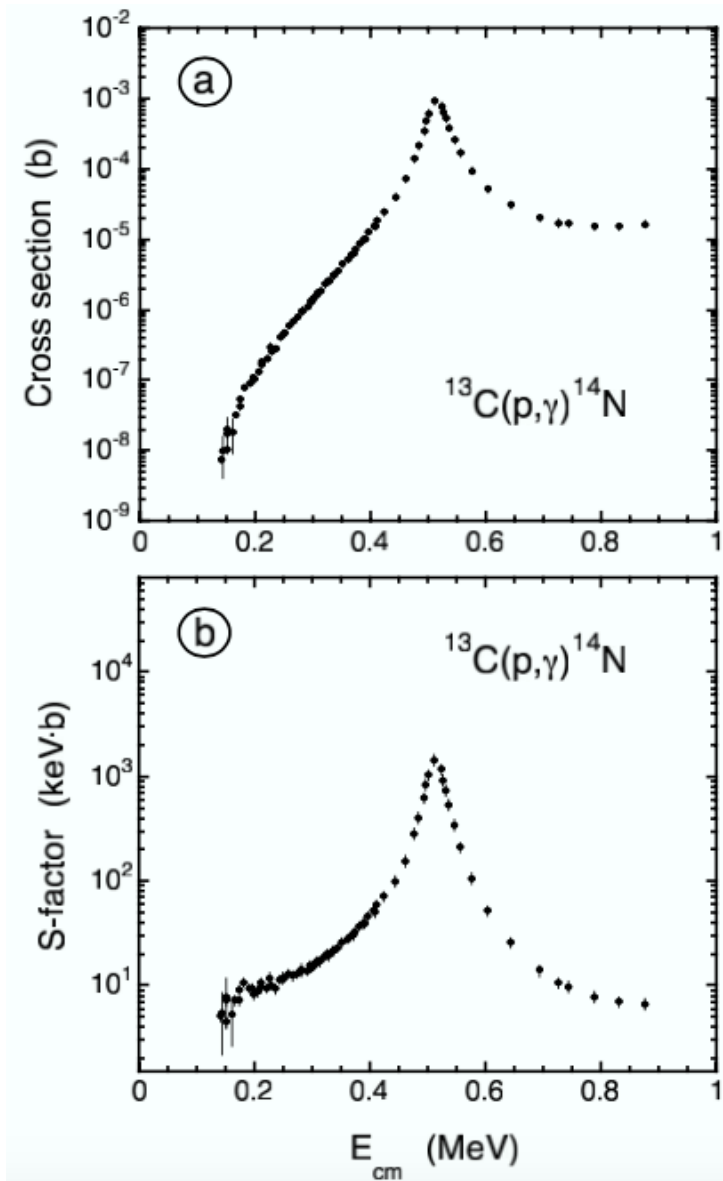
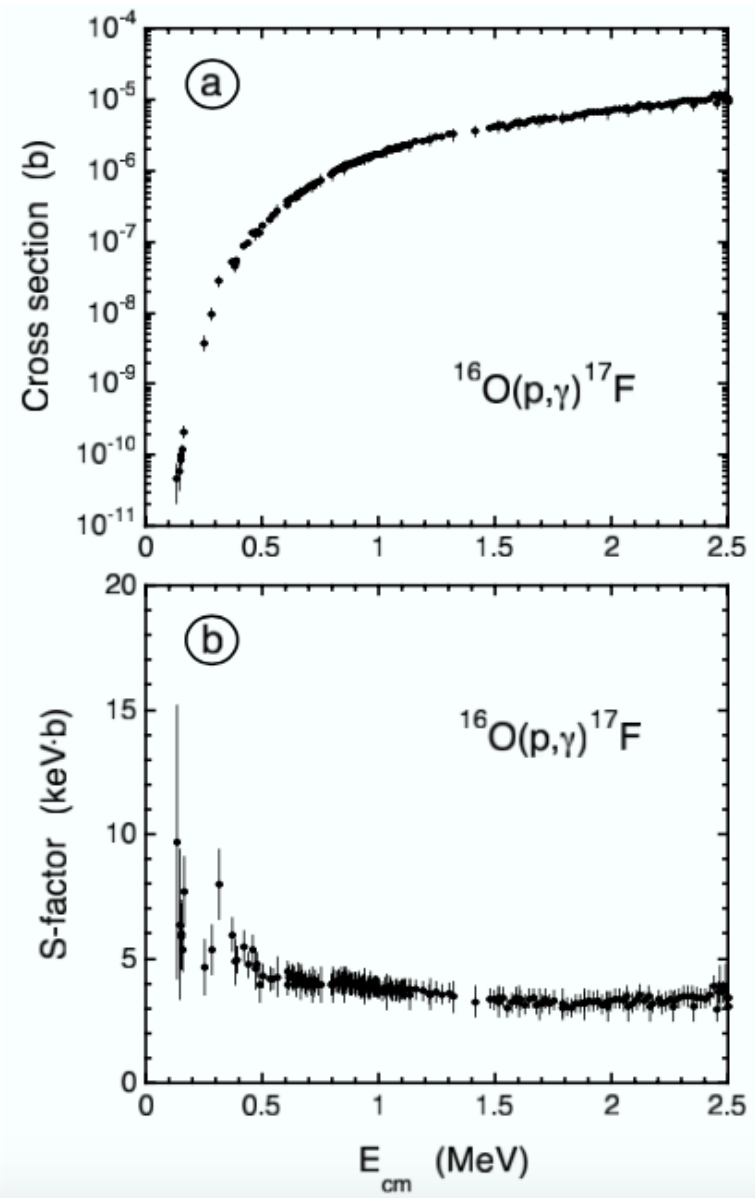
The Astrophysical S-factor contains the nuclear physics contribution to the cross section, and usually varies smoothly (and slowly) with energy.

If the angular momentum is non zero, the centrifugal barrier must also be taken into account.

There is no new physics in the astrophysical S-factor. We are just dividing out known contributions to the cross section.

As $S(E)$ is fairly constant, it is much easier to extrapolate to lower energies than the cross section, and easier to study any variations.

Cross section --> Astrophysical S-factor



From Iliadis.

Resonant reactions

Many/most of the reactions of interest proceed through the formation of a compound nucleus.

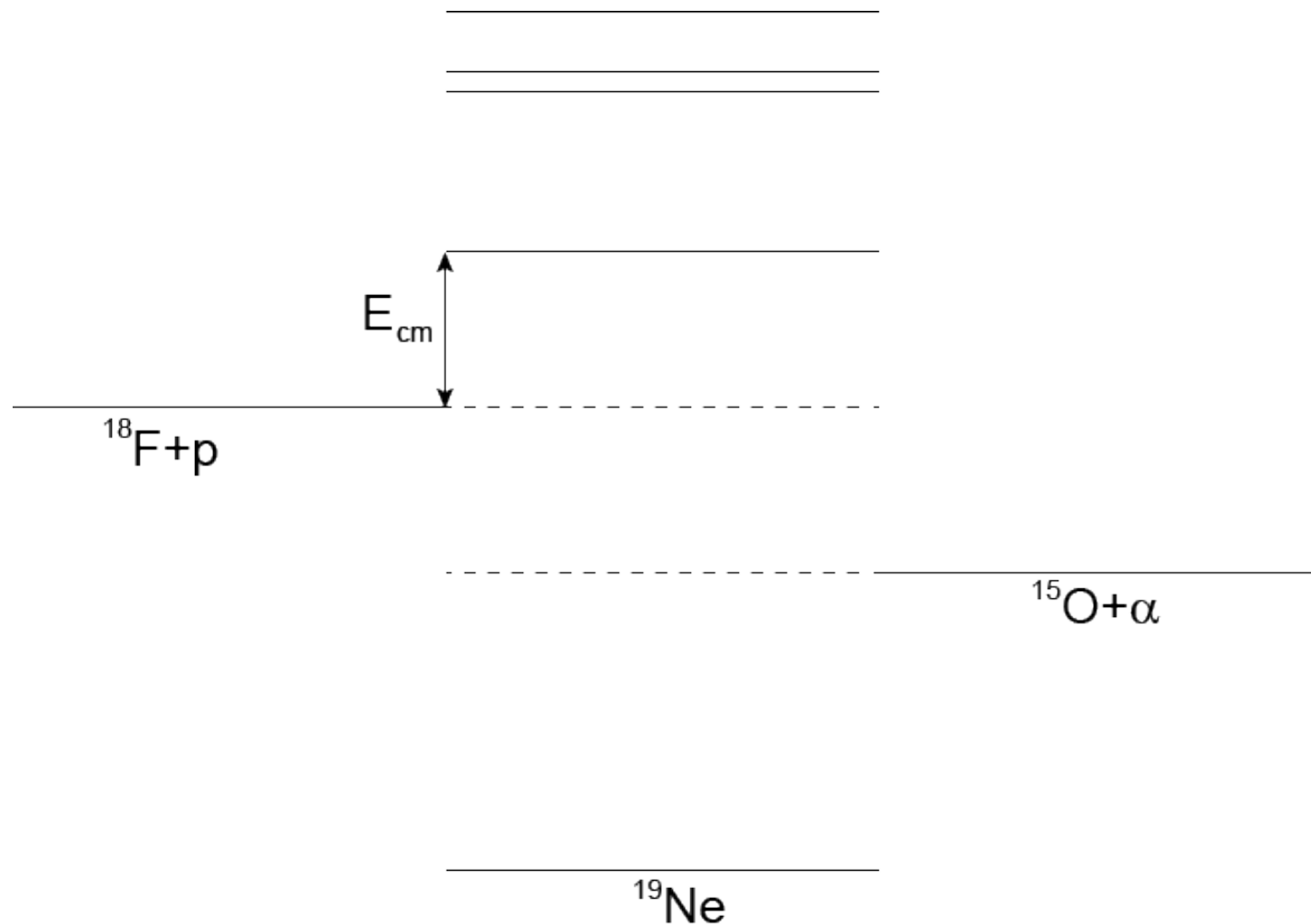
The energy range populated in the compound nucleus depends on the entrance channel Q-value and the E_{CM} (remember interesting E_{CM} range is the Gamow window).

If the compound nucleus has excited state/s in this range, then the reaction rate will have a resonant contribution:

- this resonant contribution usually dominates significantly, i.e. non-resonant (direct capture) reaction rates are much lower
- $S(E)$ is no longer a smoothly varying function with energy, but shows large increases (resonance) at particular energies => resonance
- the rate depends very sensitively on the properties of the corresponding state.

Resonant reactions are extremely important in nuclear astrophysics.

Key assumption: **compound nucleus retains no memory of its formation.**



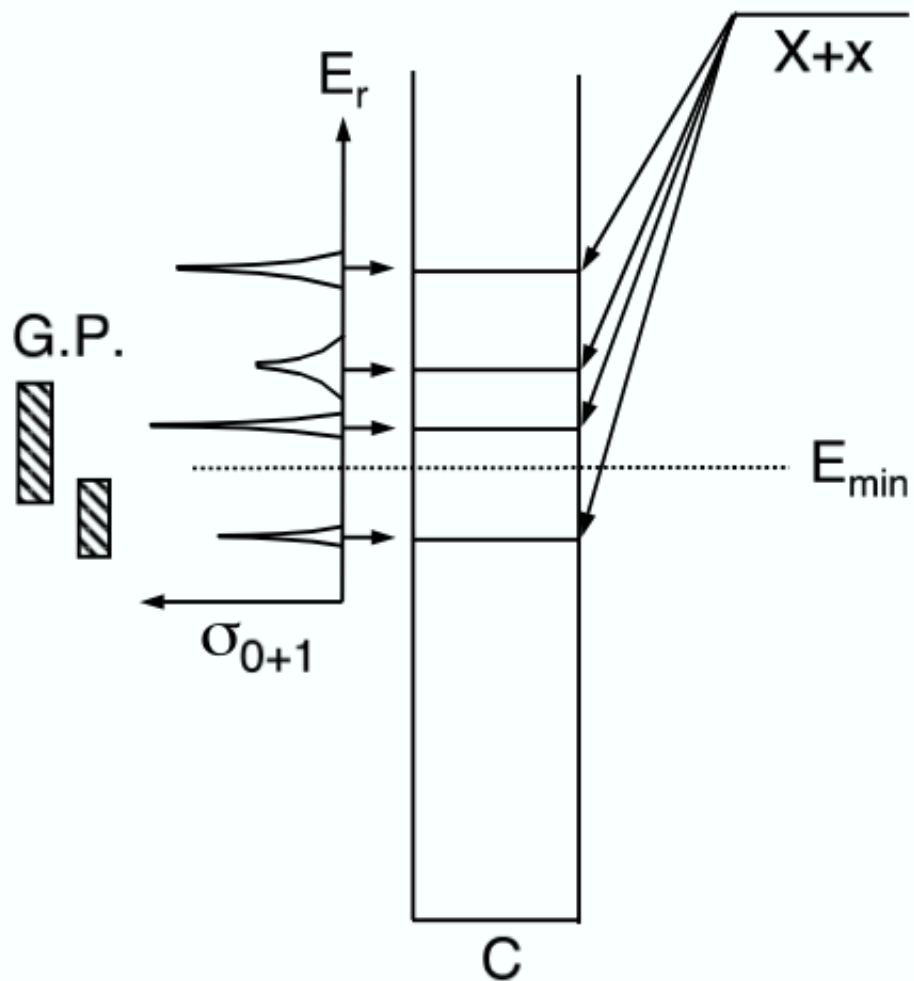


Fig. 3.25 Energy level diagram, showing narrow resonances in the reaction $0 + 1$ (left-hand side) and the corresponding levels in the compound nucleus C . The locations of two Gamow peaks at different temperatures are displayed as hatched bars. Below an energy of E_{\min} (dotted line) charged-particle measurements are not feasible. In this case one may estimate the reaction rates by measuring nuclear structure properties of levels in nucleus C via a reaction $X + x$.

From Iliadis.

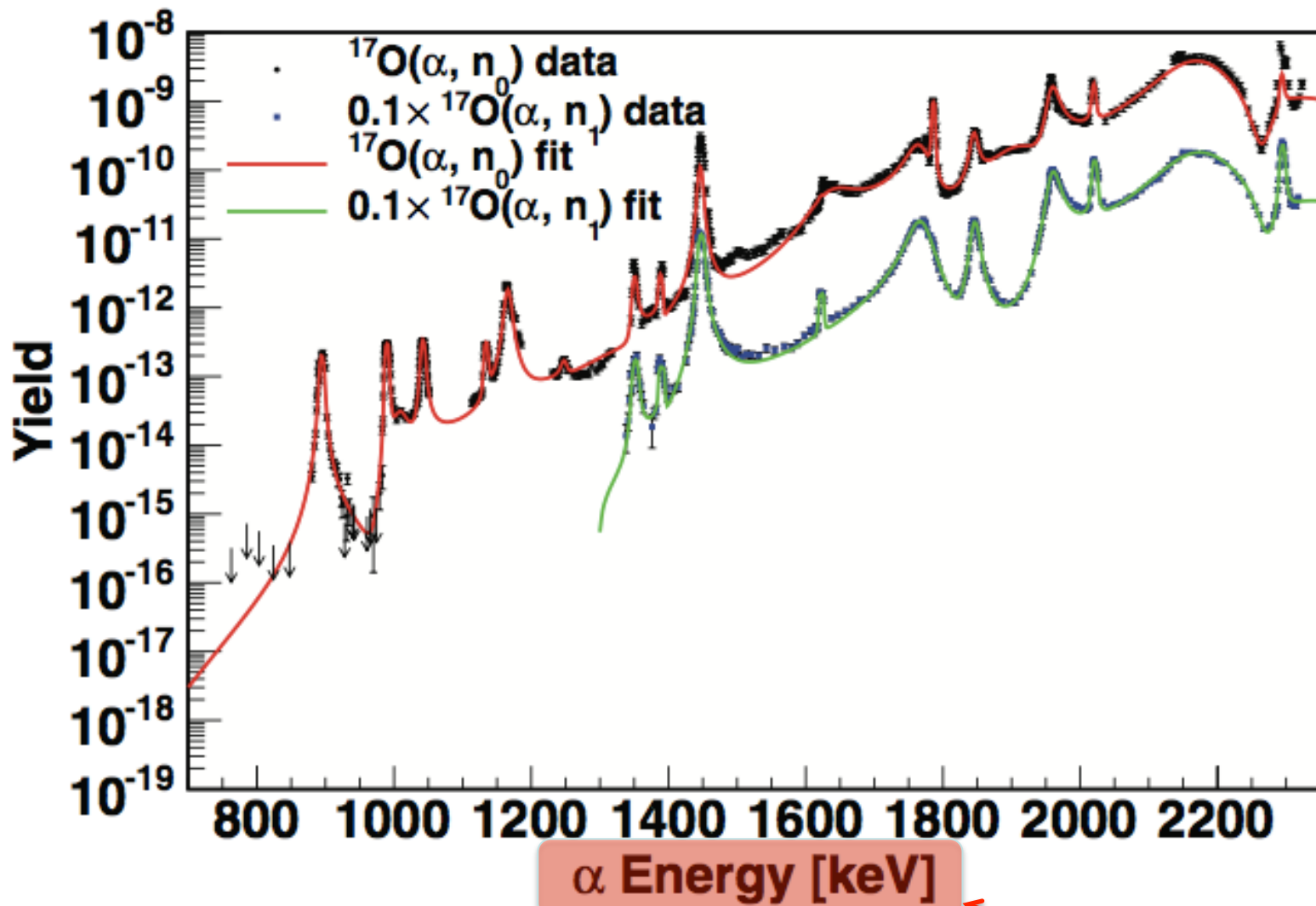


FIG. 9. (Color online) Experimental and calculated yield of the $^{17}\text{O}(\alpha, n_0)^{20}\text{Ne}$ and $^{17}\text{O}(\alpha, n_1\gamma)^{20}\text{Ne}$ reaction channels. The lines through the data points are the result of an R -matrix fit to both channels. The n_1 channel has been divided by a factor of 10 to better separate it from the n_0 plot. The arrows denote upper limits.

Best et al., Phys. Rev C 87,
045805 (2013)

Not in E_{cm}
(health warning!!)

Each resonance in previous graph corresponds to a state in the compound nucleus.

For example, state at 8.062 MeV

$$\Rightarrow E_{cm} = 8.062 -$$

$$\Rightarrow \quad =$$

Note:

$$E_{lab} = (m_T + m_P) E_{cm} / m_T$$

$$= 21/17 *$$

$$= 0.882 \text{ MeV}$$

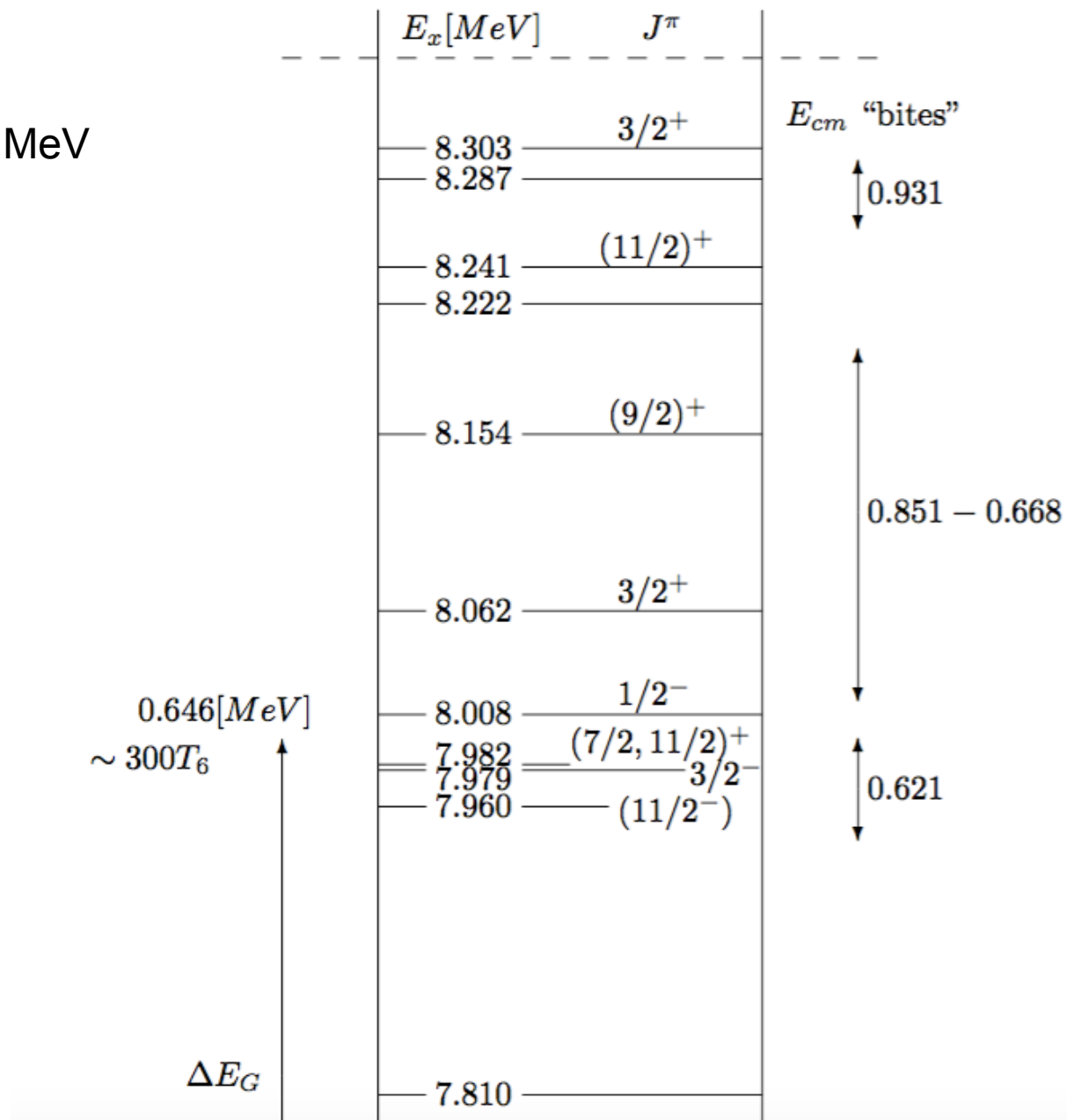
^{17}O is $J^\pi =$

Alpha is =

So s-wave =>

p-wave =>

Compound Nucleus ^{21}Ne



If we consider narrow, isolated resonances, we can describe the resonant cross section according to the Breit-Wigner formula:

$$\sigma_{BW}(E) = \frac{\lambda^2 \omega}{4\pi} \frac{\Gamma_i \Gamma_o}{(E_r - E)^2 + \Gamma^2 / 4}$$

where E_r is the resonance energy (in the centre of mass, not the E_x);

Γ is total width and related to lifetime ($\Gamma = \hbar/\tau$)

$$\Gamma = \Gamma_1 + \Gamma_2 (+ \Gamma_3 + \dots) \text{ if other possible decays}$$

Γ_i and Γ_o are the partial widths of the entrance and exit channels

Reaction rate per particle pair becomes:

$$\langle \sigma v \rangle = \left(\frac{8}{\pi \mu} \right)^{1/2} \frac{1}{(kT)^{3/2}} \int_0^\infty \sigma_{BW}(E) E \exp[-E/kT] dE$$

If resonance narrow (usual case) Maxwell-Boltzmann term doesn't change across resonance, so comes out of integral

$$\int_0^{\infty} \sigma_{BW}(E)dE = 2\pi^2 \lambda_R^2 \omega \frac{\Gamma_a \Gamma_b}{\Gamma}$$

$$\omega = \frac{2J_R + 1}{(2J_T + 1)(2J_P + 1)}$$

Spin factor

$$\omega\gamma = \omega \frac{\Gamma_a \Gamma_b}{\Gamma}$$

Resonance strength

$$\langle\sigma v\rangle = \left(\frac{2\pi}{\mu kT}\right)^{3/2} \hbar^2 (\omega\gamma) \exp(-E_R/kT)$$

If several resonances play a role, total reaction rate is sum of individual contributions.

For broad resonances, numerical integration is required.

Key points on narrow resonance formula

$$\langle \sigma v \rangle = \left(\frac{2\pi}{\mu kT} \right)^{3/2} \hbar^2 (\omega\gamma) \exp(-E_R/kT)$$

- Only need to know **resonance energy** and **strength** (*these are properties of the state and do not depend on the reaction*).
- $\omega\gamma$ is proportional to area under resonance cross section
- Γ_n and Γ_γ not very sensitive to resonance energy
- Γ_p and Γ_α very sensitive to resonance energy \rightarrow transmission probability
- Consider low lying resonance in e.g. (α,γ) reaction
 - $\Gamma_\gamma \gg \Gamma_\alpha$
 - So $\gamma = \Gamma_\gamma \cdot \Gamma_\alpha / \Gamma = \Gamma_\gamma \cdot \Gamma_\alpha / \Gamma_\gamma = \Gamma_\alpha$

Where one partial width is much smaller than the other, it dominates the rate (*assuming only two open channels*).
But of course it is hardest to measure!

Example – helium burning: triple α process

Step 1: two alpha particles \longleftrightarrow ^8Be

^8Be is unstable ($Q = -92 \text{ keV}$) and decays back to two alpha particles with a lifetime of $1 \times 10^{-16} \text{ s}$. However, this is long enough for a small concentration to build up (for $T_6 = 100$, $\rho = 10^5 \text{ g/cm}^3$, one ^8Be for every 10^9 alpha particles).

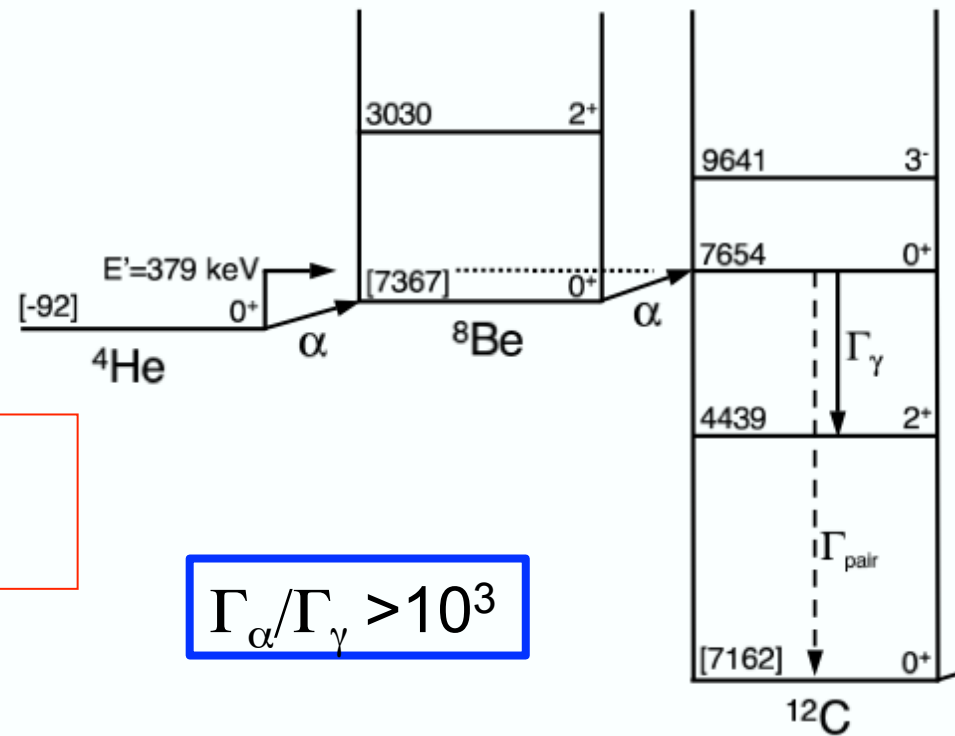
Step 2: $^8\text{Be} + ^4\text{He} \longleftrightarrow ^{12}\text{C}$

Step 1 provides sufficient ^8Be for there to be a small but non-negligible rate of alpha capture to ^{12}C . This stage is also weak as the ^{12}C is formed at high excitation energies and preferentially decays back to $^8\text{Be} + ^4\text{He}$.

However, this rate is still too small to explain the carbon abundance. This realisation led Hoyle (Yorkshire astronomer!) to make probably the most successful prediction of nuclear astrophysics.

He suggested that to explain the observed carbon abundance, there should be an **s-wave resonance in ^{12}C** near the $^8\text{Be} + ^4\text{He}$ threshold (resonant capture) at around 7.7 MeV Ex.

This prediction prompted significant experimental effort. In 1957 Cook, Fowler, Lauritsen and Lauritsen at Kellogg Radiation Laboratory at Caltech discovered a state with the correct properties (at 7.654 MeV).



If this state did not exist, neither would we!

$$\Gamma_\alpha / \Gamma_\gamma > 10^3$$

The combined effect of these two steps is to turn three alpha particles into a ^{12}C – the triple alpha process.

Figure from Iliadis.



Basic formula and terminology

Cross section – probability for reaction to occur

$$\text{No. of reactions (yield)} = N_i N_t \sigma \varepsilon$$

N_i = number of incident particles

N_t = number of target particles/unit area

ε = efficiency

And remember centre of mass to lab energy conversion

$$E_{cm} = E_{lab} m_T / (m_T + m_p)$$

Forward kinematics: light beam on heavy target

(most older measurements are light beams – data often plotted in E_p/E_α not E_{cm})

Inverse kinematics: heavy beam on light target

Direct and Indirect methods

There are two methods we can use to experimentally determine the information we need to calculate a reaction rate.

Direct ‘direct’ measurement of the relevant cross section or resonance strength

Spectroscopic measurement of nuclear parameters to allow cross section or resonance strength to be calculated (i.e. energy, spin/parity, width, partial width)

Direct Measurements

Advantages:

- Measurement of reaction rate in as close to real conditions as currently possible
- Independent of models

Disadvantages:

- Small cross sections
 - Low yield
 - High background
- Beam/target availability
- Sometimes it's just too hard!

Indirect Measurements

Advantages

- Many more options available
- Wider choice of beam/target combination
- Typically higher cross sections
- Usually fewer background issues

Disadvantages

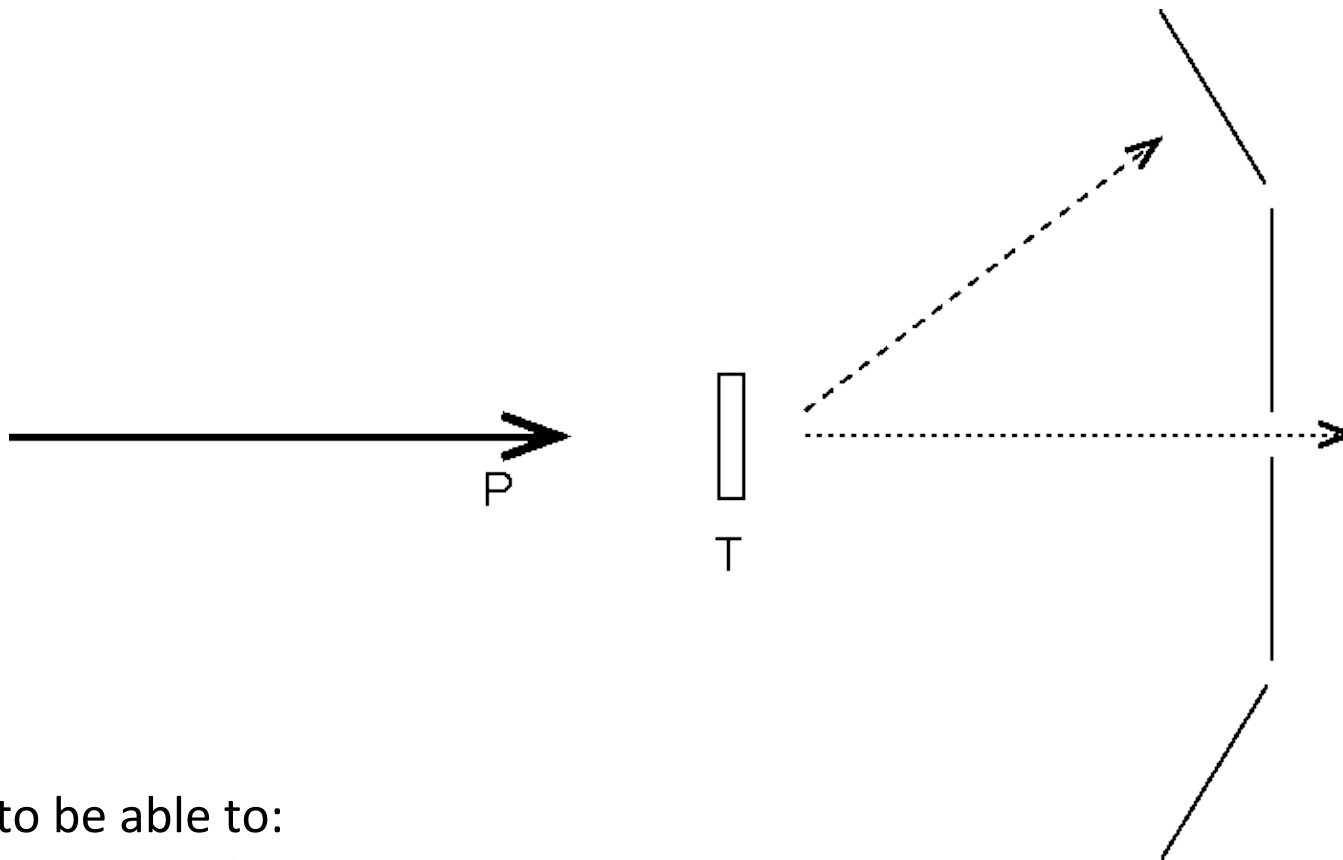
- Model dependent
 - Implicit assumptions
 - Applicability
 - Interpretation
 - Other data required

Indirect techniques

Common techniques to extract spectroscopic information
(*energy, total width, partial widths, spins*):

- Transfer reactions
 - alpha transfer
 - (d,p) reactions
 - (${}^3\text{He}$,d) reactions
- Time reverse
 - Detailed balance if direct not feasible
- Activation
 - Measure decays offline
- Gamma spectroscopy

Schematic of experiment



We need to be able to:

- ✧ Determine N_i and N_t
- ✧ Determine efficiency
- ✧ **Unambiguously** identify events of interest from everything else detected – reaction yield

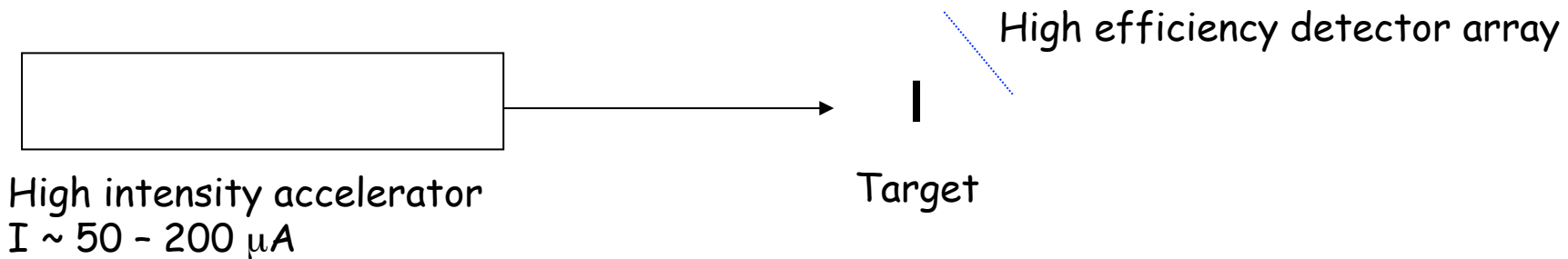
Information usually available: energy, time of flight, position, angle, particle type.

5. Direct measurements

5. Direct measurements

5.i Forward kinematics measurements

Forward kinematics - stable beams



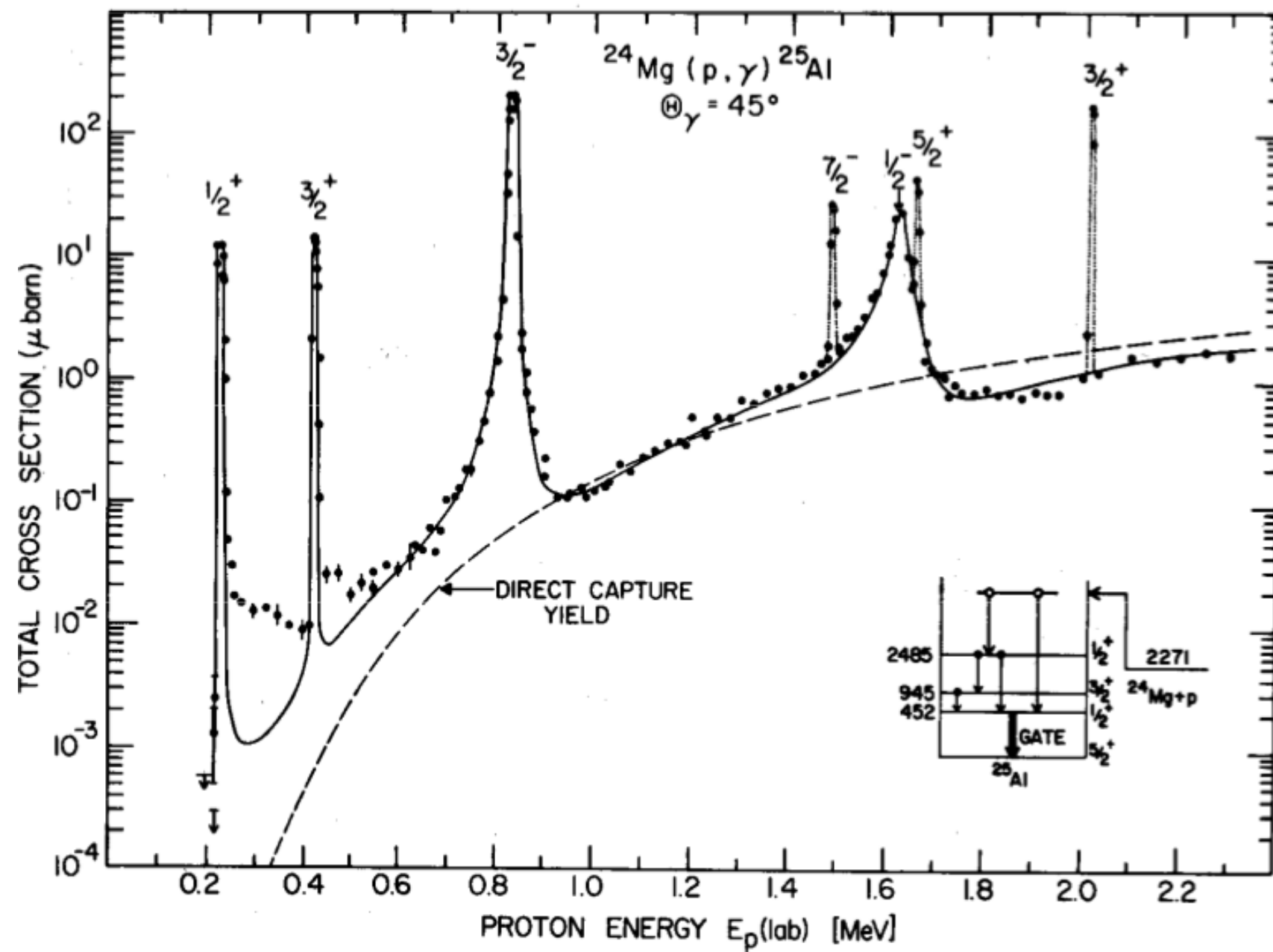
$$100 \mu A + 100 \mu g/cm^2 + 4\pi \text{ coverage} + 100\% \text{ efficient} \rightarrow 1/s (\text{nb})$$

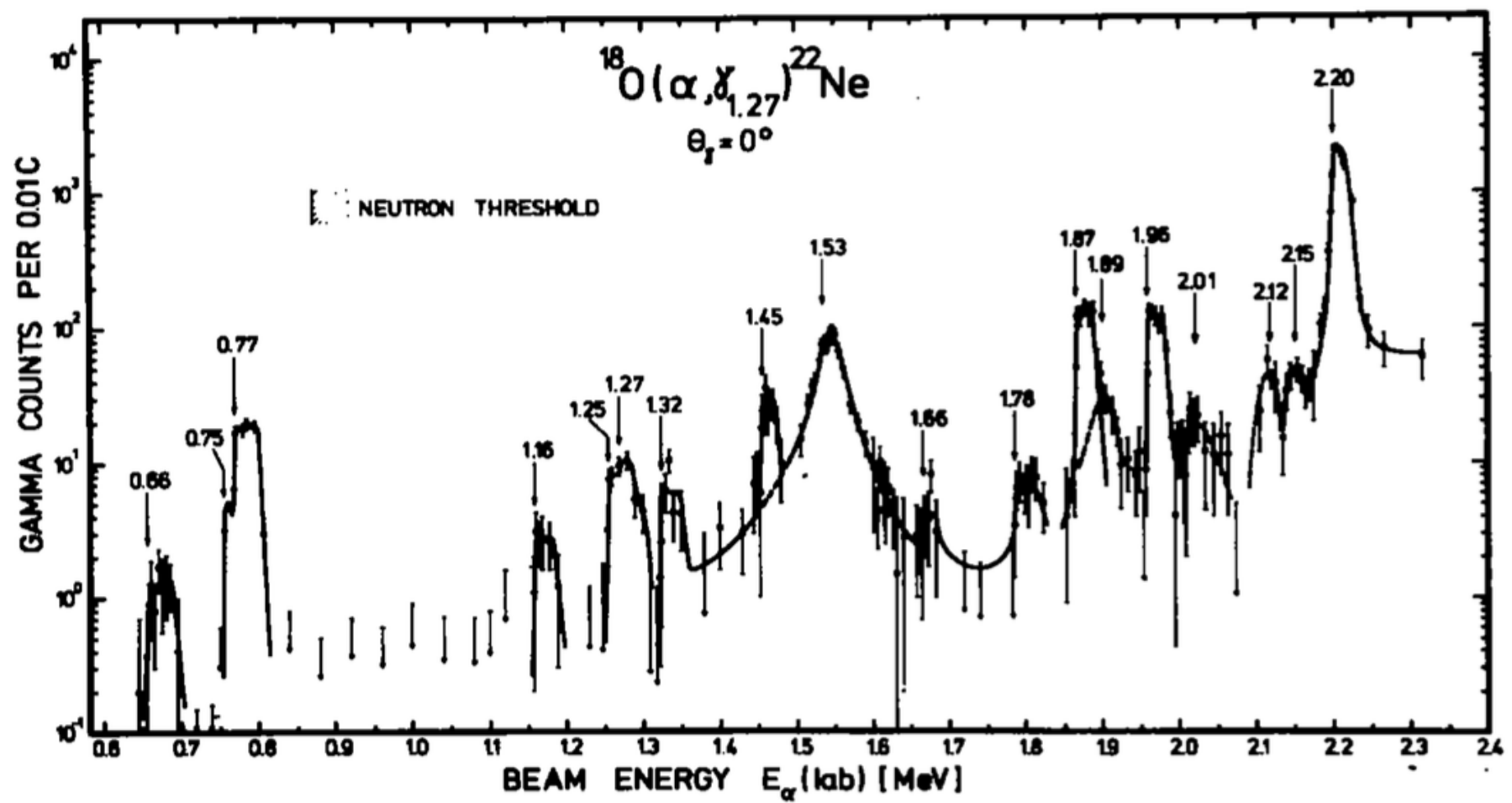
Benefits

- High beam intensity
- Fast energy changes

Challenges

- recoil usually does not leave target (have to do in singles)
- background from impurities on target and window – need to know target
- products come out at all angles
- for radiative capture, need to know branching ratios and angular distributions





$^{23}\text{Na}(\alpha, p)$ – Aarhus University, Denmark

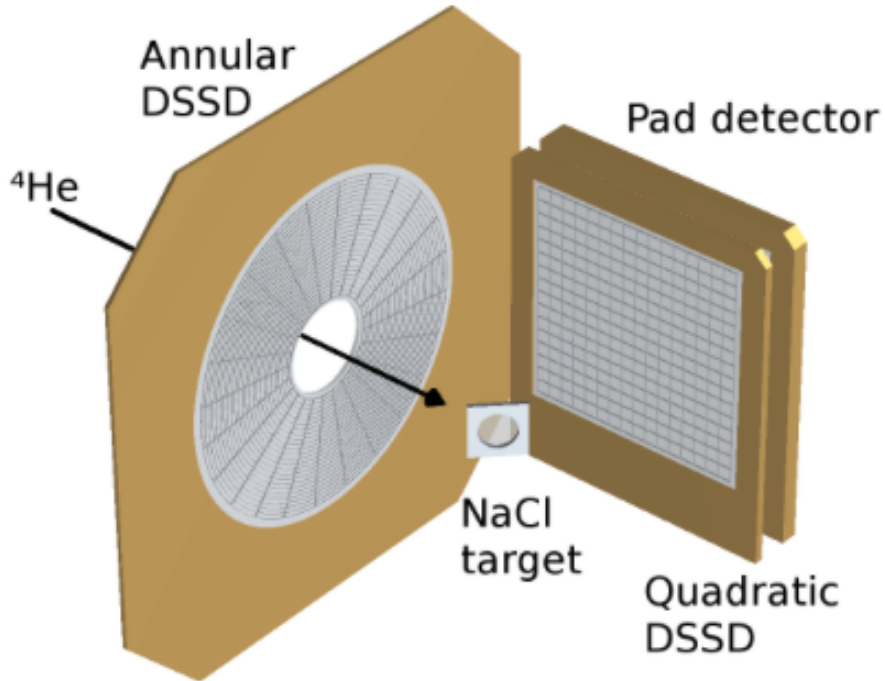


FIG. 1. A schematic of the experimental setup within the scattering chamber. The incoming ^4He beam is indicated by the arrow. The NaCl target was orientated at 45° relative to the beam axis. Two double-sided silicon strip detectors were used to detect outgoing protons and α particles, see the text for details. For clarity both front- and back-side segmentation of the detectors is shown.

Howard et al., PRL 2015

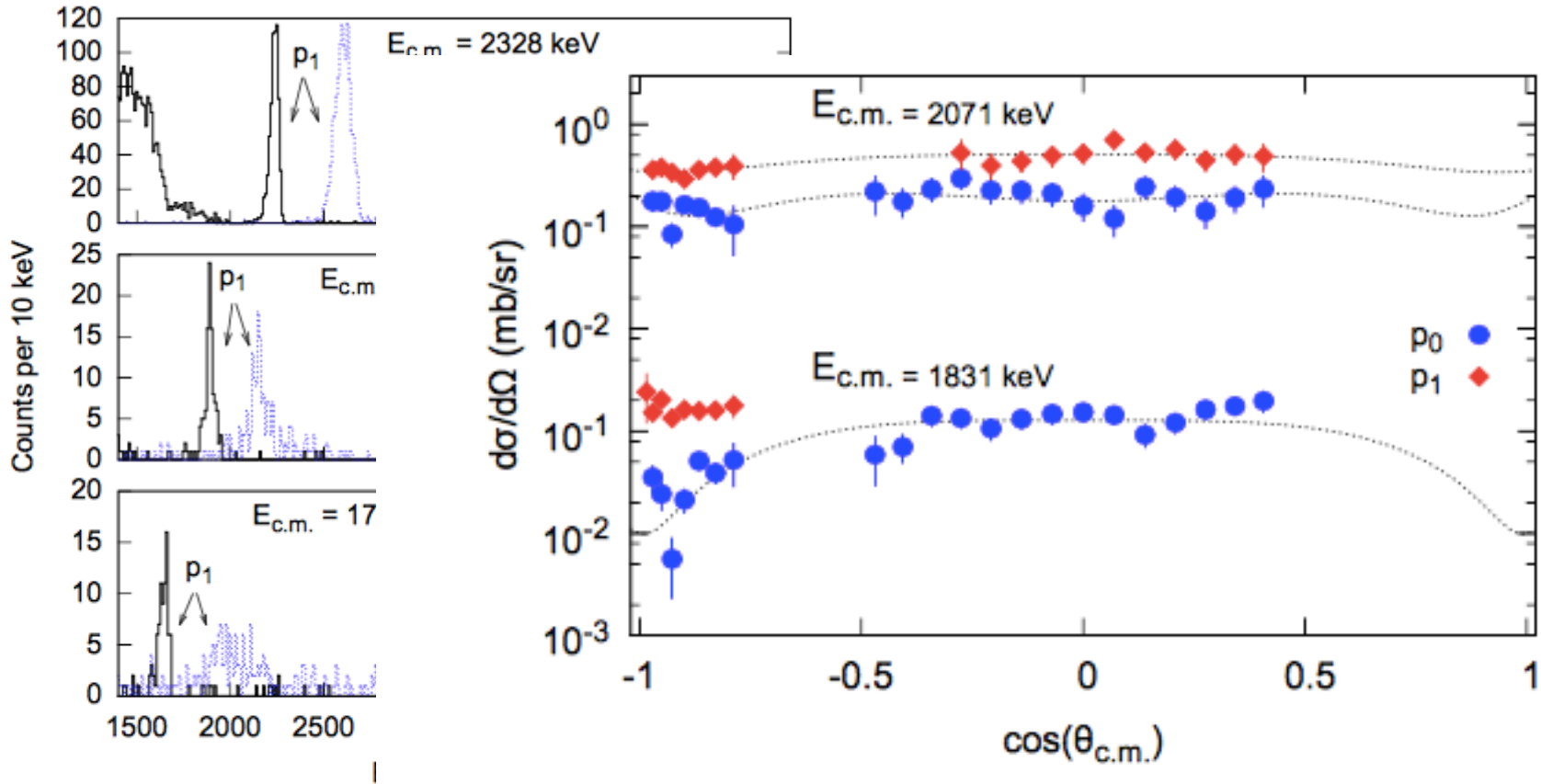
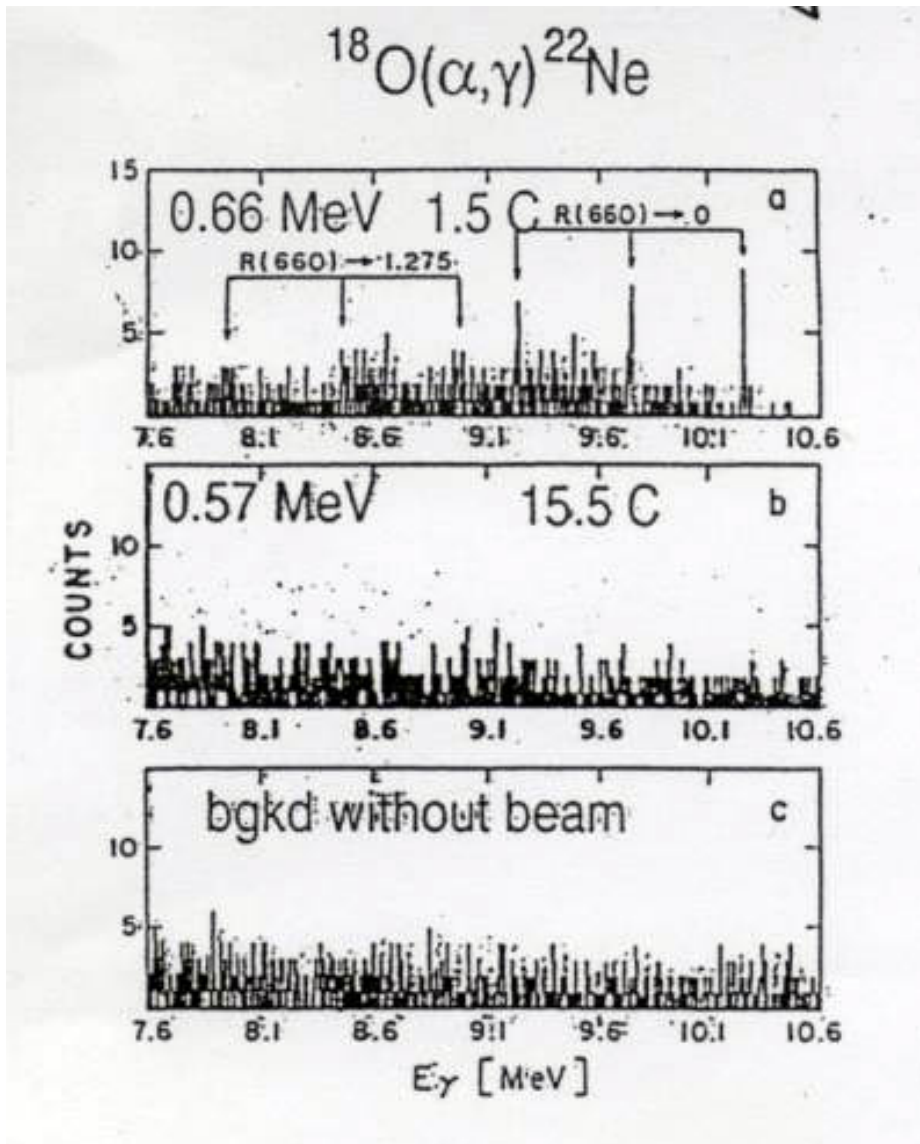


FIG. 3. Representative energy spectra from the DSSD (S3) and the quadrat scope (W1). In the latter case, the requirement to remove particles stopping in the quadrat limits the mass energy in each case is given in the caption. The small peak at the p_0 transition in $^{19}\text{F}(\alpha,p)^{20}\text{Ne}$ is indicative of a thin layer of ^{19}F . See text for further discussion.

FIG. 4. Proton angular distributions from the $^{23}\text{Na}(\alpha,p)^{26}\text{Mg}$ reaction. The energies given are the effective centre of mass energies, corrected for the target thickness. For the lowest energy p_1 data shown reliable differential cross sections could only be obtained in the annular DSSD detector, located at backward angles in the laboratory frame. The dotted lines show fits of Legendre polynomials to the data.



Reasonable measurement at
0.66 MeV

Drop 90 keV and see no counts
after 2 days

Natural background from
similar period

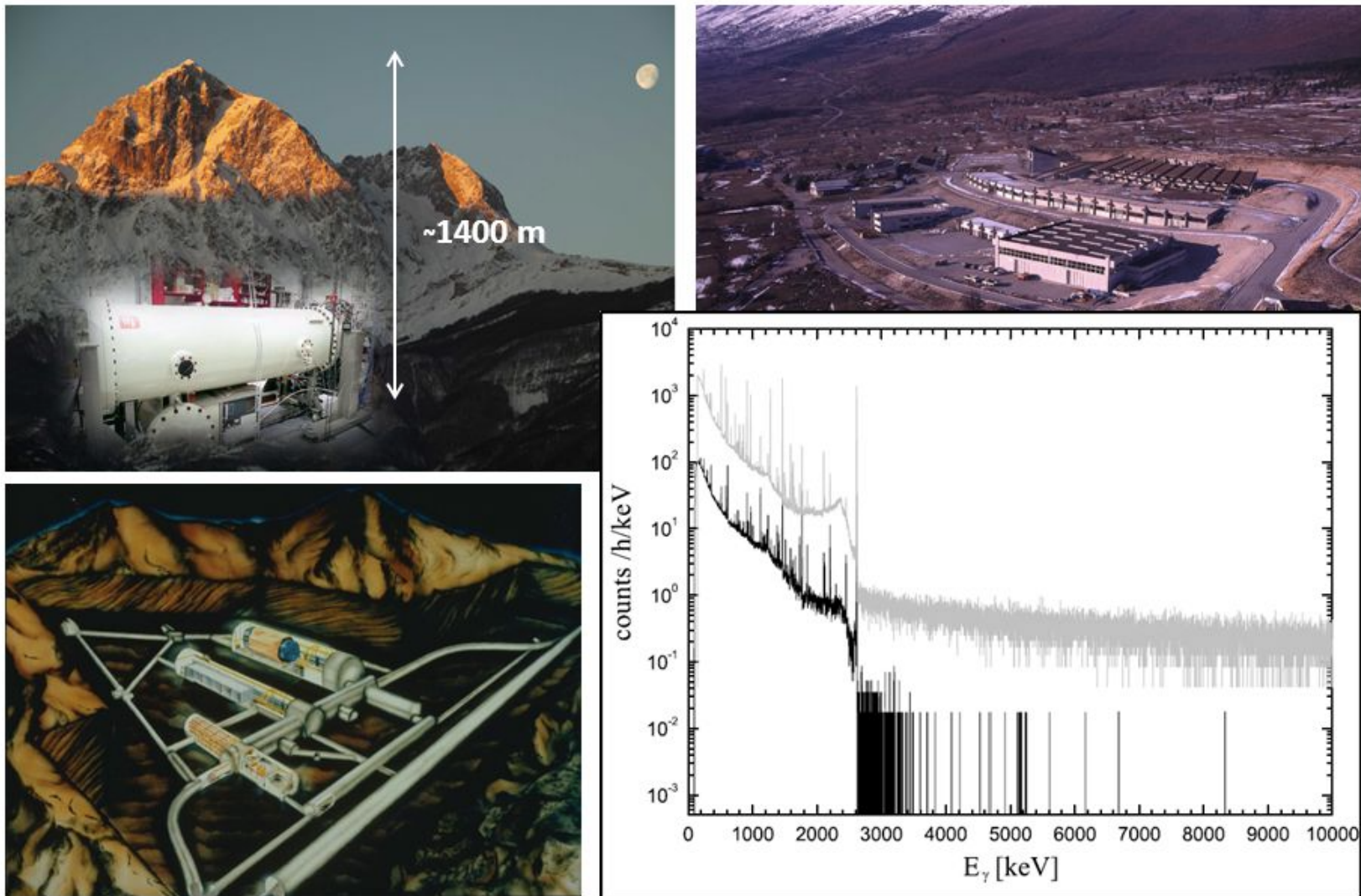
NB. Helium burning ($T_9 = 0.1 - 0.2$) $E_G \sim 250$ keV

5. Direct measurements

5.ii Underground measurements

LUNA – Laboratory for Underground Nuclear Astrophysics

Currently only facility in the world making such measurements.



Passive shielding from 1.4 km of overhead rock.

(<https://luna.lngs.infn.it>)

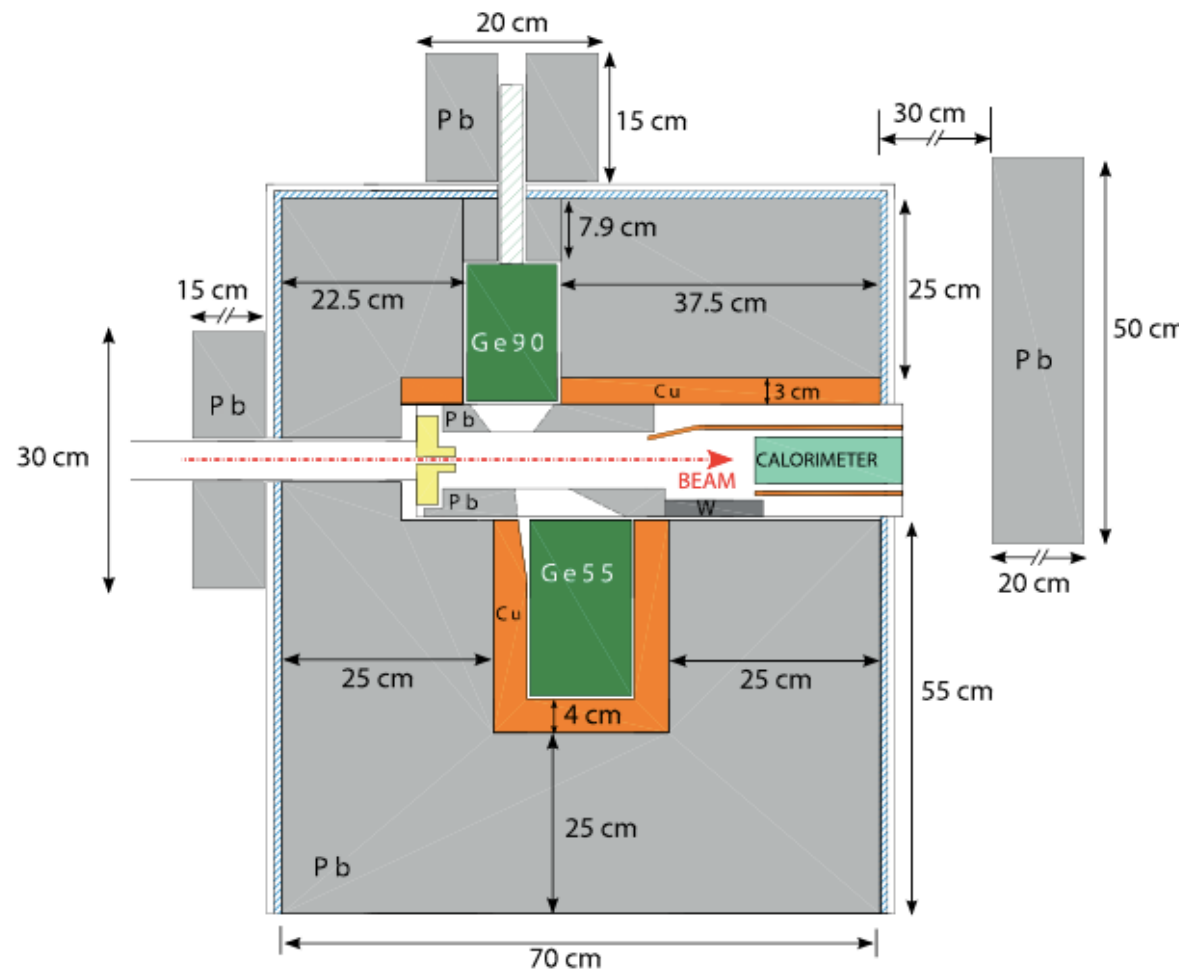


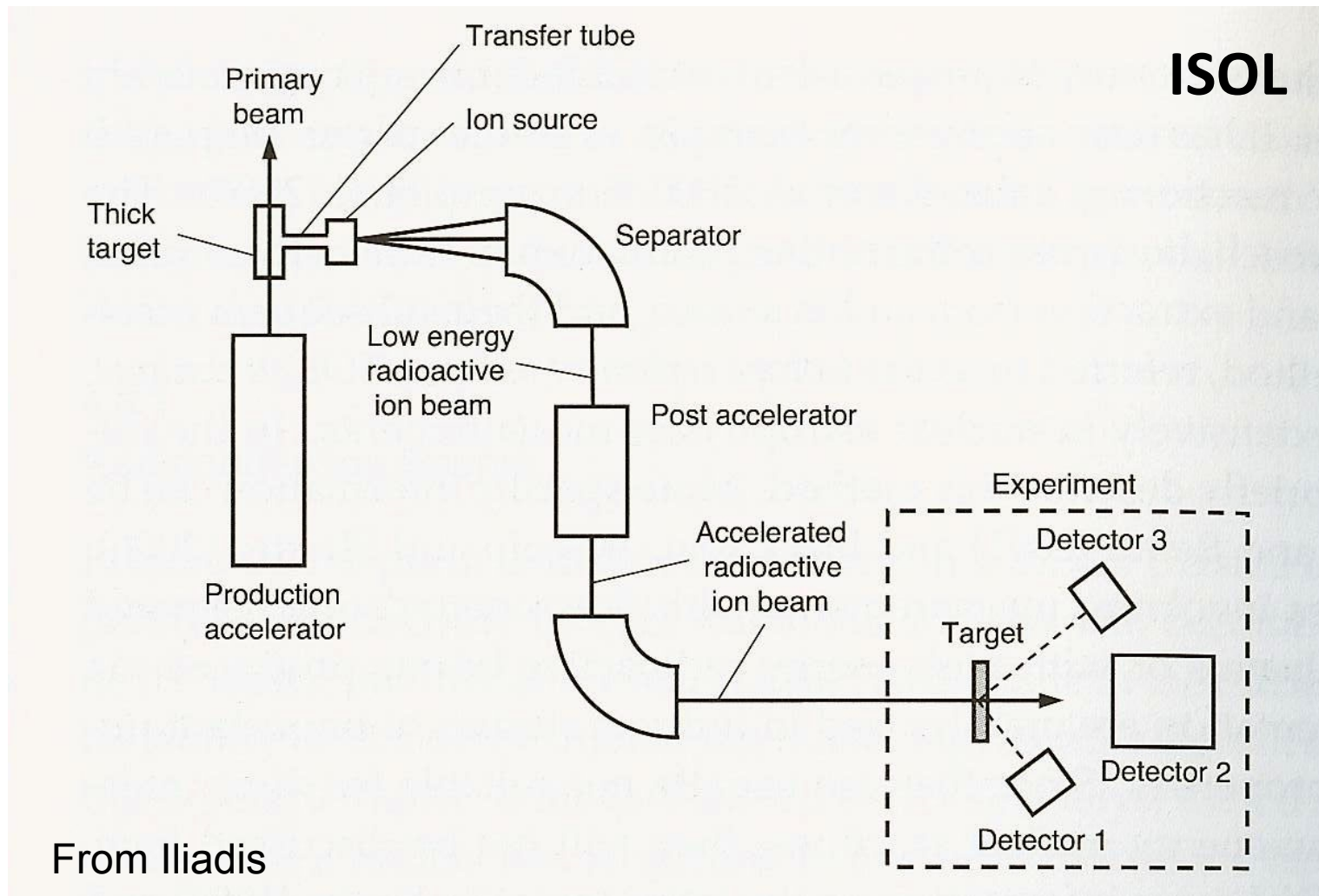
FIG. 1 (color online). Target chamber, germanium detectors (Ge55 and Ge90), and copper (orange) and lead (gray) shielding. The external lead wall on the right-hand side covers the shielding gap where the calorimeter is inserted [17–19].

5. Direct measurements

5.iii Inverse kinematics measurements

5.iii Inverse kinematics - radioactive beams

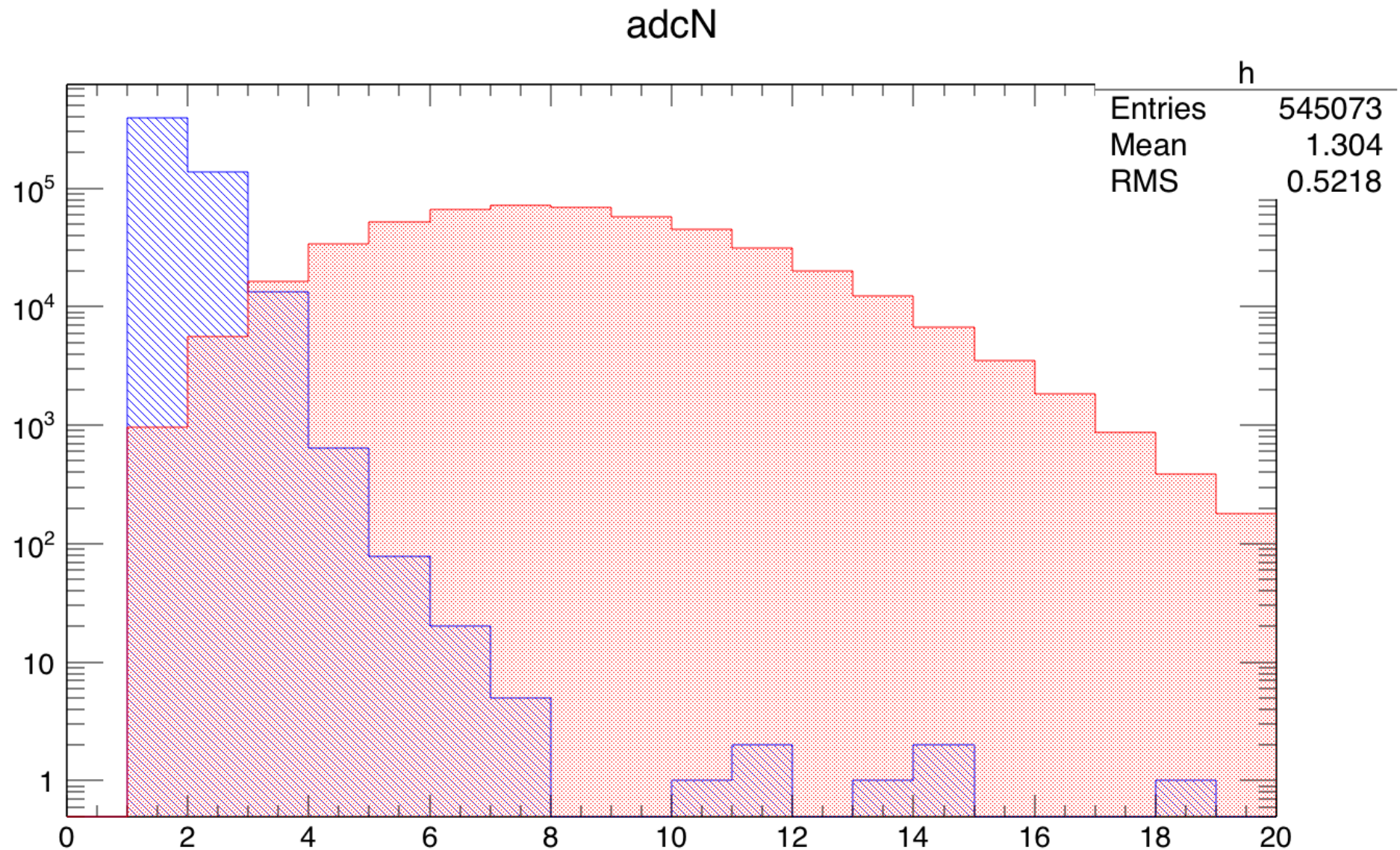
Of the two types of facility (fragmentation and ISOL) the latter are usually best for nuclear astrophysics (lower and variable energy, and better resolution)



The problem with radioactive beam...

... is that it's radioactive!

Number of hits per event (multiplicity) in silicon array
 ^{21}Ne (blue) and ^{21}Na (red) on helium cell.



Experimental challenges with radioactive beams

1. Low beam intensity

Beams typically $\times 10^6$ lower than stable beams

2. Beam induced background

If beam stops near detectors, see decay products

- High energy β s (from β -decay)
- Gammas (from decays or bremsstrahlung)
- 511s (from positron annihilation)

(a) In-flight decays

(b) Collimators

take great care here – even if only intercept 5% of beam,
would give $5 \times 10^5 \text{ s}^{-1}$ for 10^7 pps

(c) Faraday Cup

(d) Scattered beam

e.g. ^{13}N at $10^9/\text{s}$ on $100 \text{ mg/cm}^2 \text{ }^{12}\text{C}$

At 10 cm, on detector and walls have $3000/\text{s/m}^2$ at 10°
or $30/\text{s/m}^2$ at 30°

ISAC – A RIB facility

Isotope Separator and Accelerator

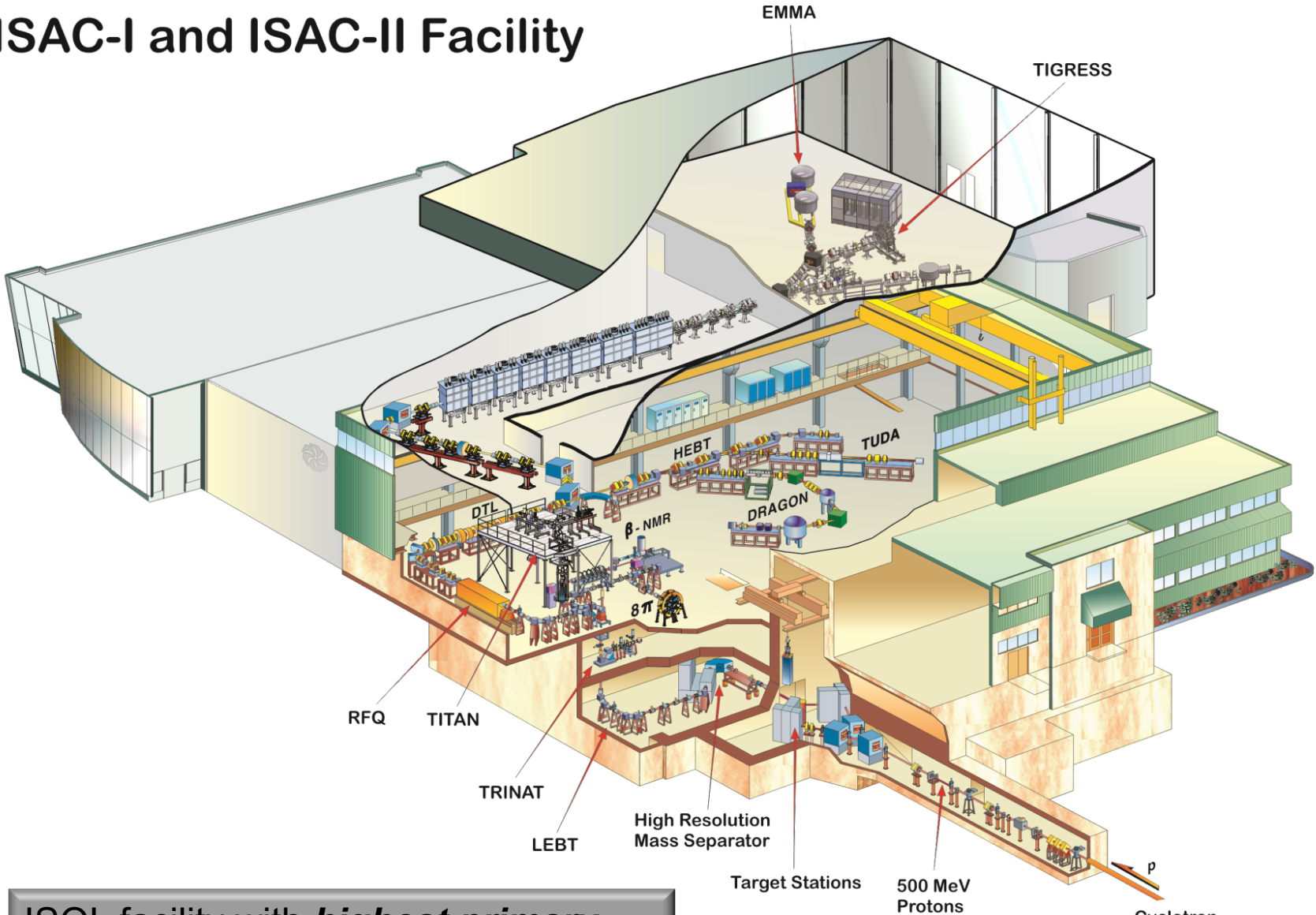
The first “purpose-built” facility for nuclear astrophysics experiments using radioactive beams

Housed in TRIUMF Laboratory in Vancouver and uses existing 500 MeV p cyclotron beam as driver

$$E = 0.15 - 1.8 \text{ MeV/u}$$

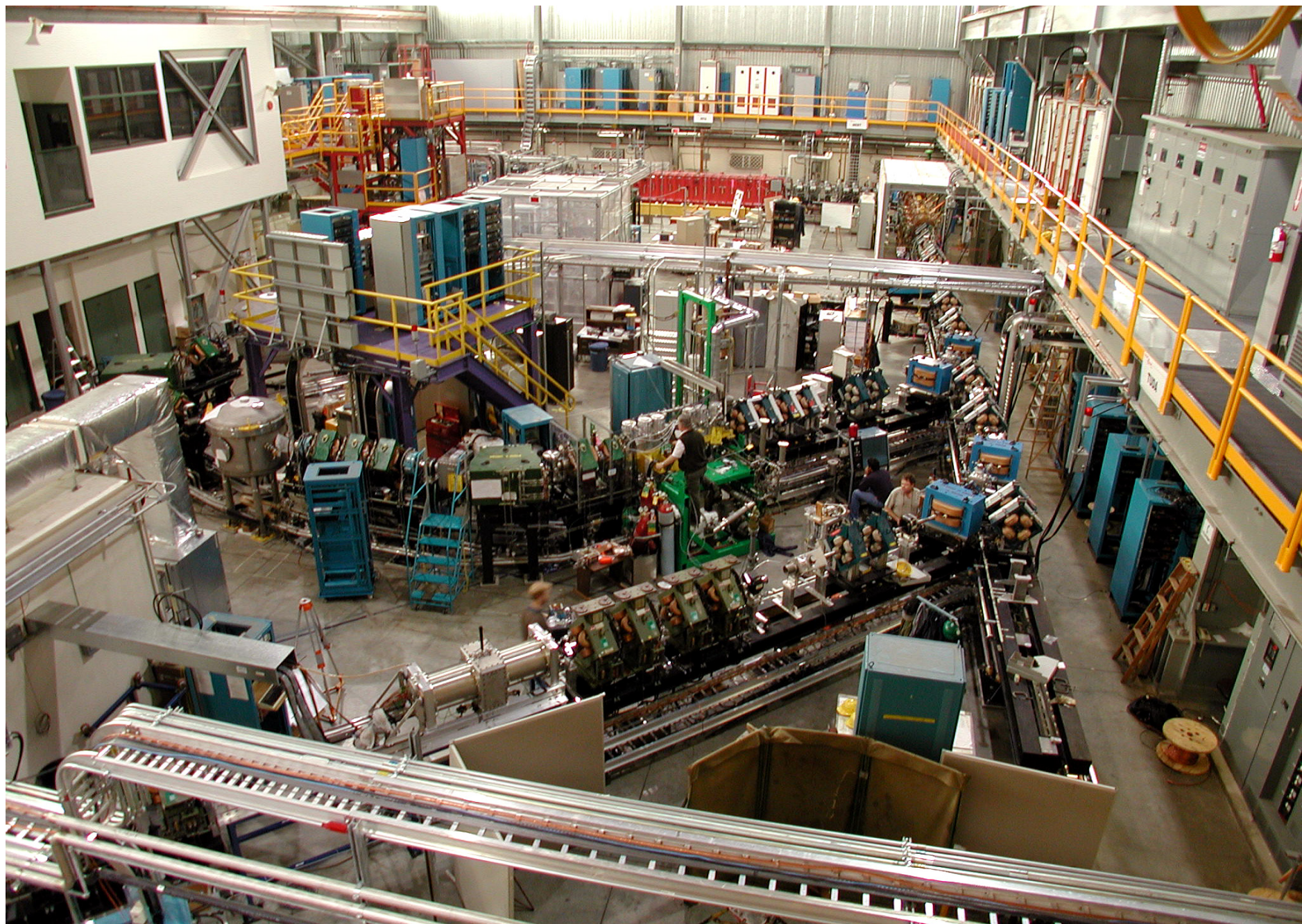
$$I = 10^5 - 10^{10} \text{ pps}$$

ISAC-I and ISAC-II Facility



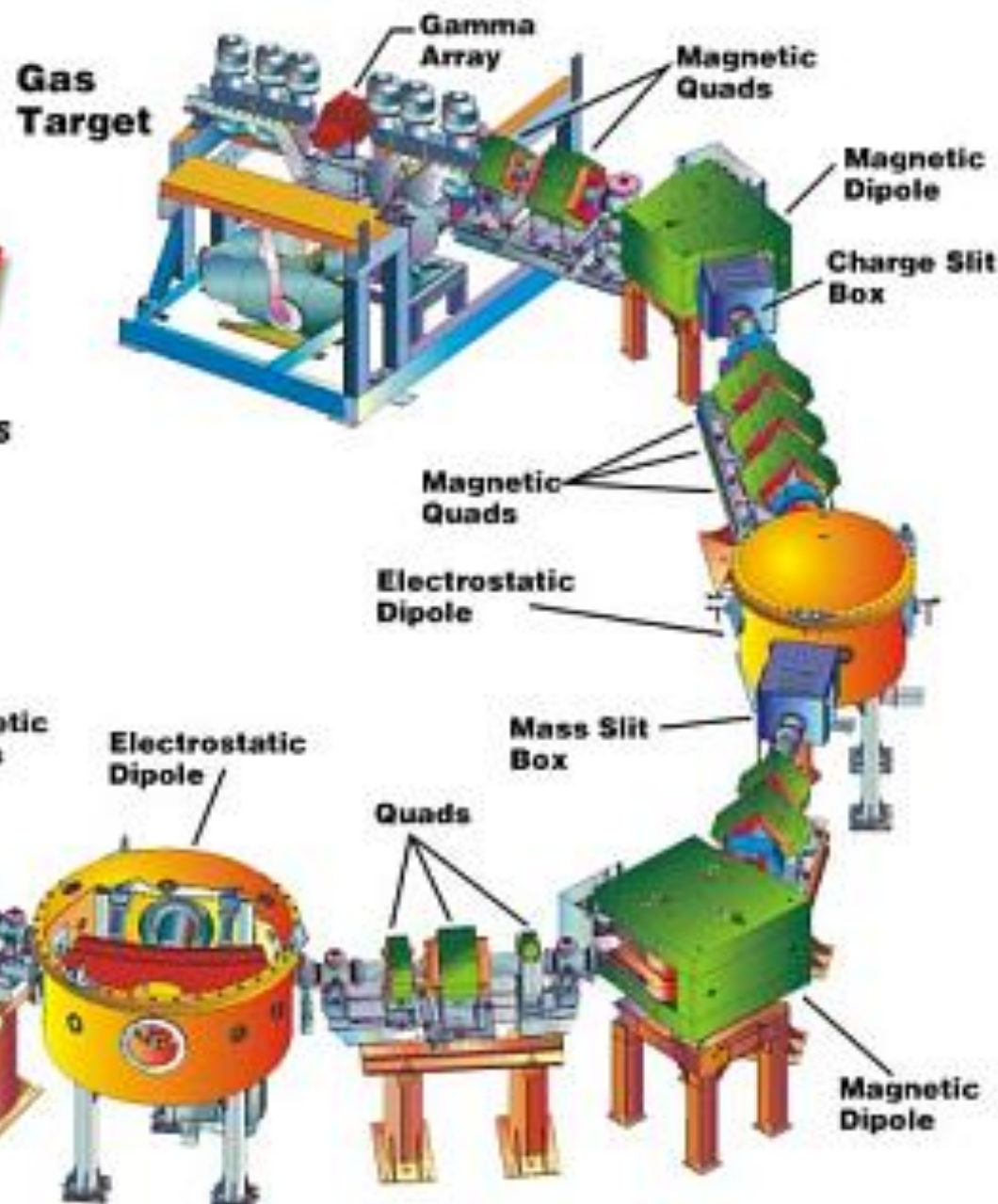
ISOL facility with ***highest primary beam intensity*** (100 μ A, 500 MeV, p)

ISOL User facility with \sim 1000 users

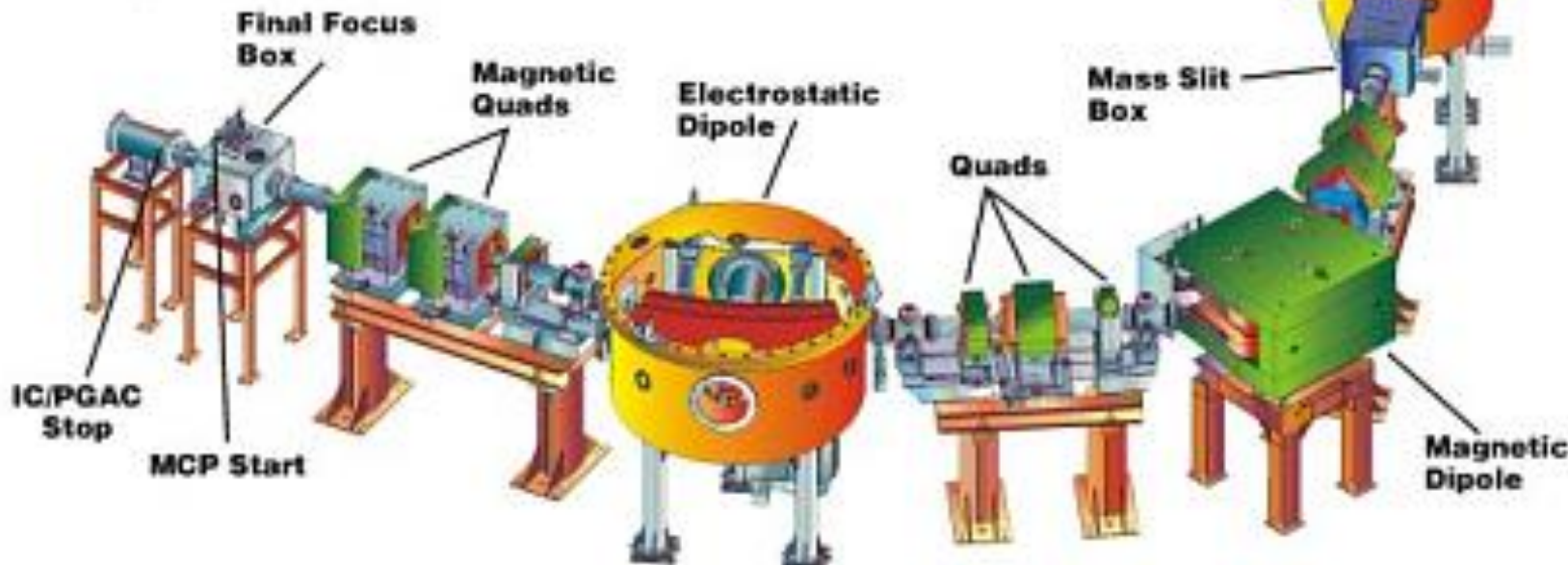


DRAGON

**Detector of Recoils And
Gammas Of Nuclear reactions**

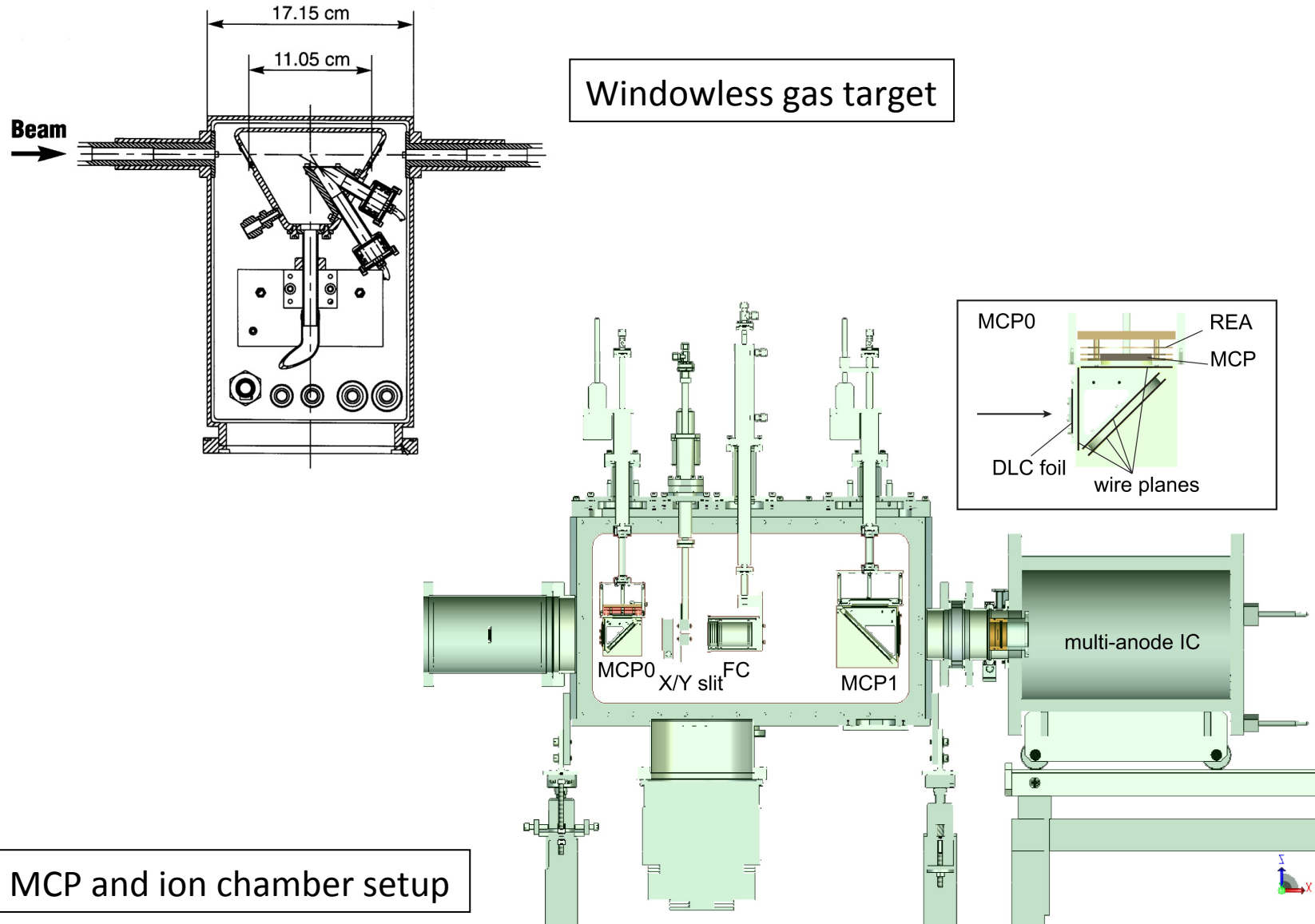


Recoil Detectors





The heart of the DRAGON

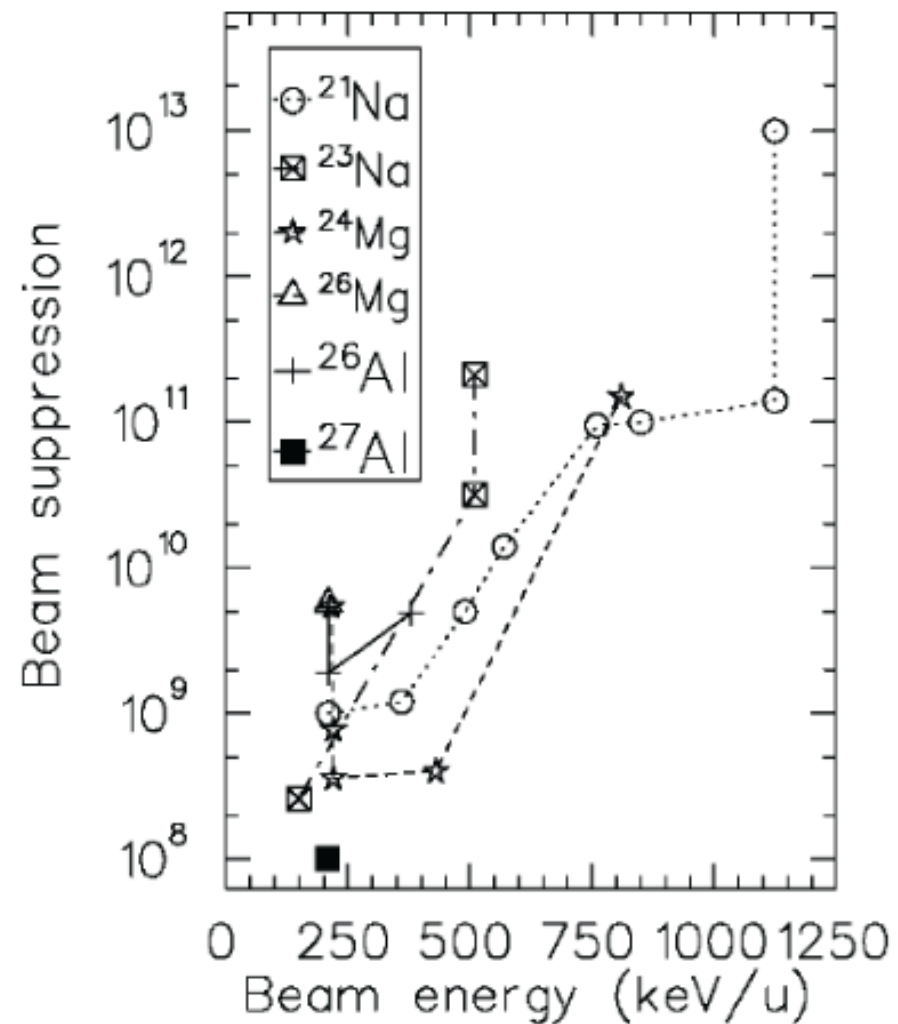


MCP and ion chamber setup

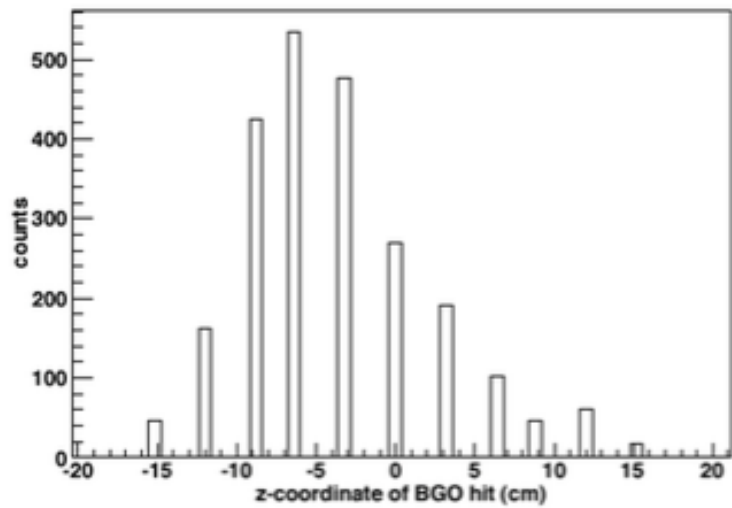
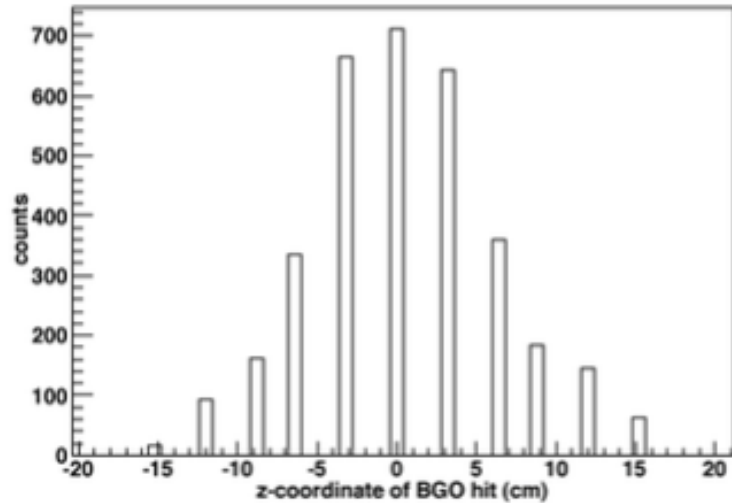
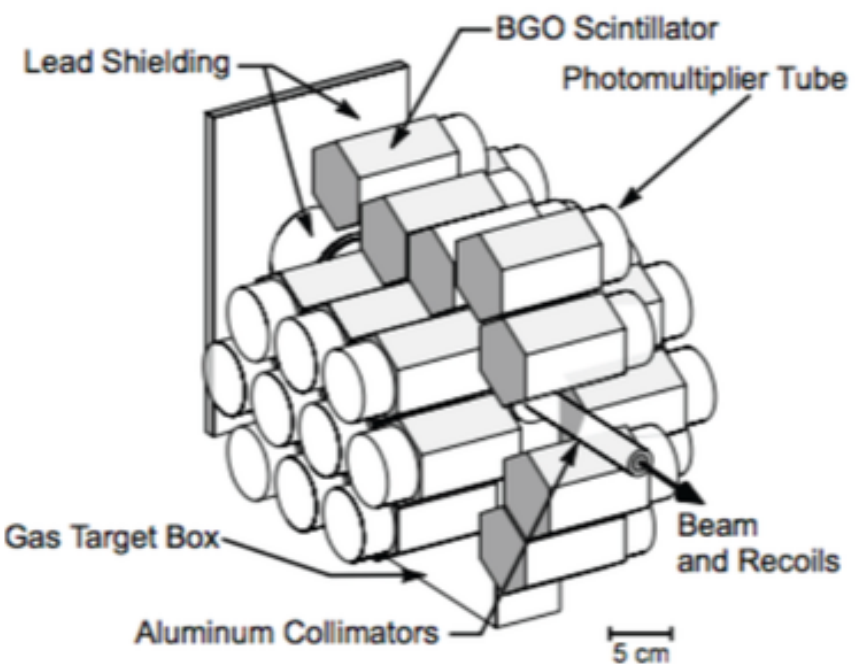
C. Vockenhuber *et al.*, NIMA 603, 372-378 (2009)

- Demonstrated suppression for (p, γ) : $10^8 - 10^{13}$
- $> 10^{14}$ raw suppression recently demonstrated^a for ${}^3\text{He}(\alpha, \gamma){}^7\text{Be}$
- γ -recoil coincidence + particle ID cuts further increase suppression

^aS. Sjue *et al.*, Nucl. Inst. Meth. A 700 179 (2013)



- 30-element $\text{Bi}_4\text{Ge}_3\text{O}_{12}$ array
- ~40% - 80% efficiency,
multiplicity & energy
dependent

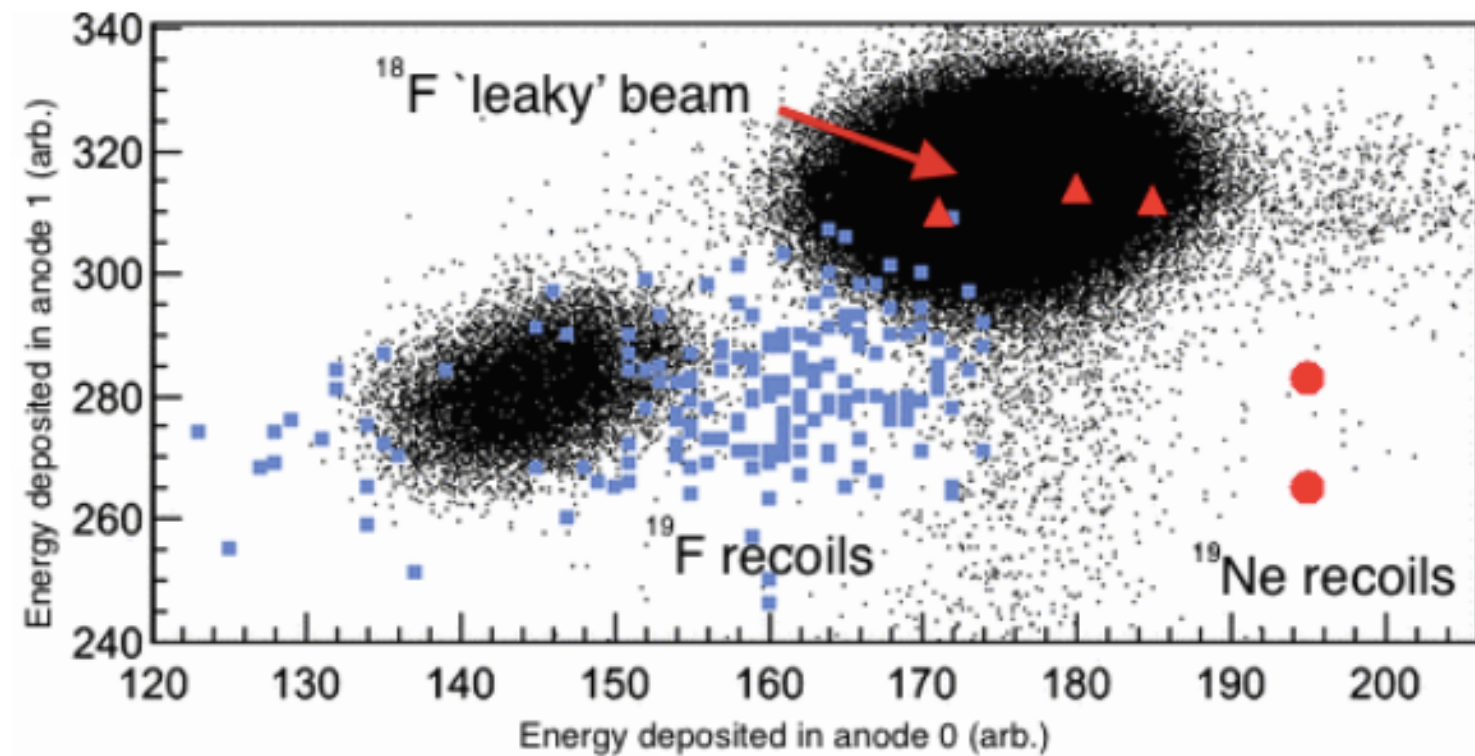


Slide from C. Ruiz

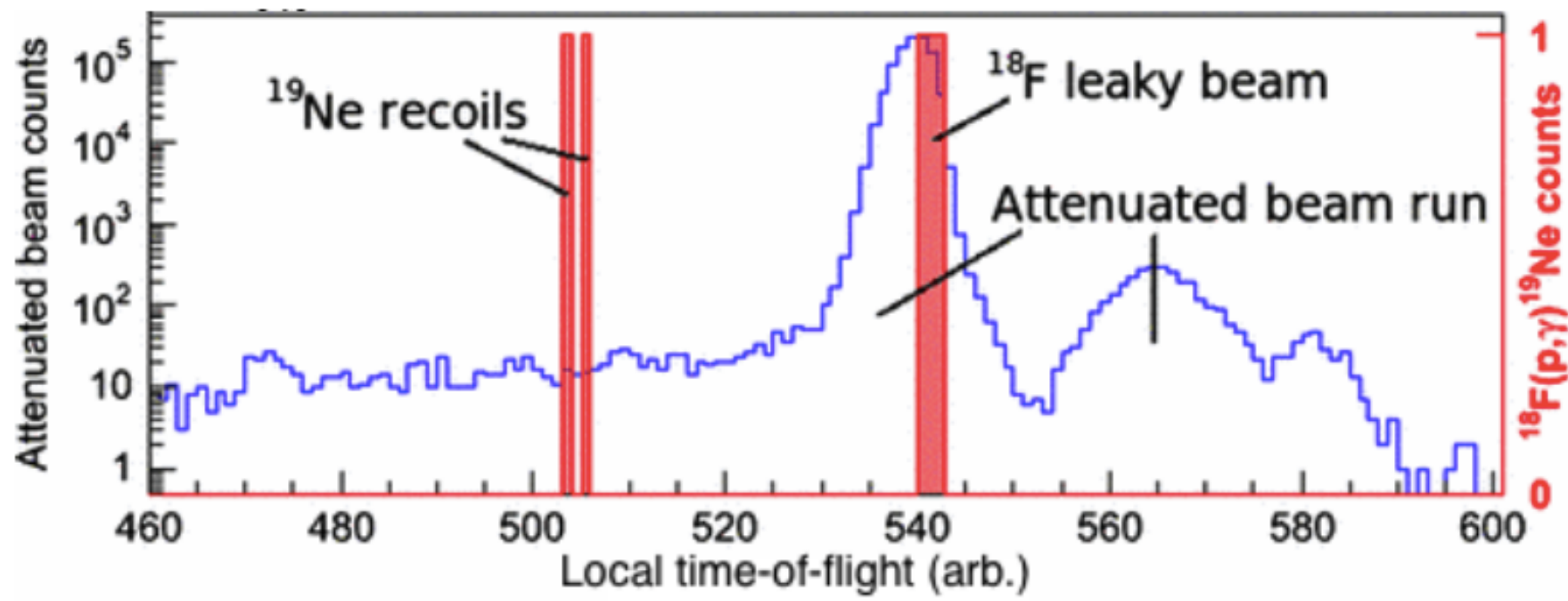
Reaction	Motivation	Intensity (s ⁻¹)	Purity (desired:contaminant)
$^{21}\text{Na}(p, \gamma)^{22}\text{Mg}$	1.275 MeV line emission in ONe novae	5×10^9	100%
$^{12}\text{C}(\alpha, \gamma)^{16}\text{O}$	Helium burning in red giants	3×10^{11}	
$^{26g}\text{Al}(p, \gamma)^{27}\text{Si}$	Nova contribution to galactic ^{26}Al	3×10^9	30,000:1
$^{12}\text{C}(^{12}\text{C}, \gamma)^{24}\text{Mg}$	Nuclear cluster models	3×10^{11}	
$^{40}\text{Ca}(\alpha, \gamma)^{44}\text{Ti}$	Production of ^{44}Ti in SNII	3×10^{11}	10,000:1 - 200:1
$^{12}\text{C}(^{16}\text{O}, \gamma)^{28}\text{Si}$	Nuclear cluster models	3×10^{11}	
$^{23}\text{Mg}(p, \gamma)^{24}\text{Al}$	1.275 MeV line emission in ONe novae	5×10^7	1:20 - 1:1,000
$^{17}\text{O}(\alpha, \gamma)^{21}\text{Ne}$	Neutron poison in massive stars	1×10^{12}	
$^{18}\text{F}(p, \gamma)^{19}\text{Ne}$	511 keV line emission in ONe novae	2×10^6	100:1
$^{33}\text{S}(p, \gamma)^{34}\text{Cl}$	S isotopic ratios in nova grains	1×10^{10}	
$^{16}\text{O}(\alpha, \gamma)^{20}\text{Ne}$	Stellar helium burning	1×10^{12}	
$^{17}\text{O}(p, \gamma)^{18}\text{F}$	Explosive H burning in novae	1×10^{12}	
$^3\text{He}(\alpha, \gamma)^7\text{Be}$	Solar neutrino spectrum	5×10^{11}	
$^{58}\text{Ni}(p, \gamma)^{59}\text{Cu}$	High mass tests (p-process, XRB)	6×10^9	
$^{26m}\text{Al}(p, \gamma)^{27}\text{Si}$	SNII contribution to galactic ^{26}Al	2×10^5	1:10,000
$^{38}\text{K}(p, \gamma)^{39}\text{Ca}$	Ca/K/Ar production in novae	2×10^7	1:1
$^{19}\text{Ne}(p, \gamma)^{20}\text{Na}$	F production	1×10^7	1:1
$^{22}\text{Ne}(p, \gamma)^{23}\text{Na}$	Na production	1×10^{12}	

$^{18}\text{F}(\text{p},\gamma)^{19}\text{Ne}$ – lowest beam intensity at DRAGON

Particle ID spectra:



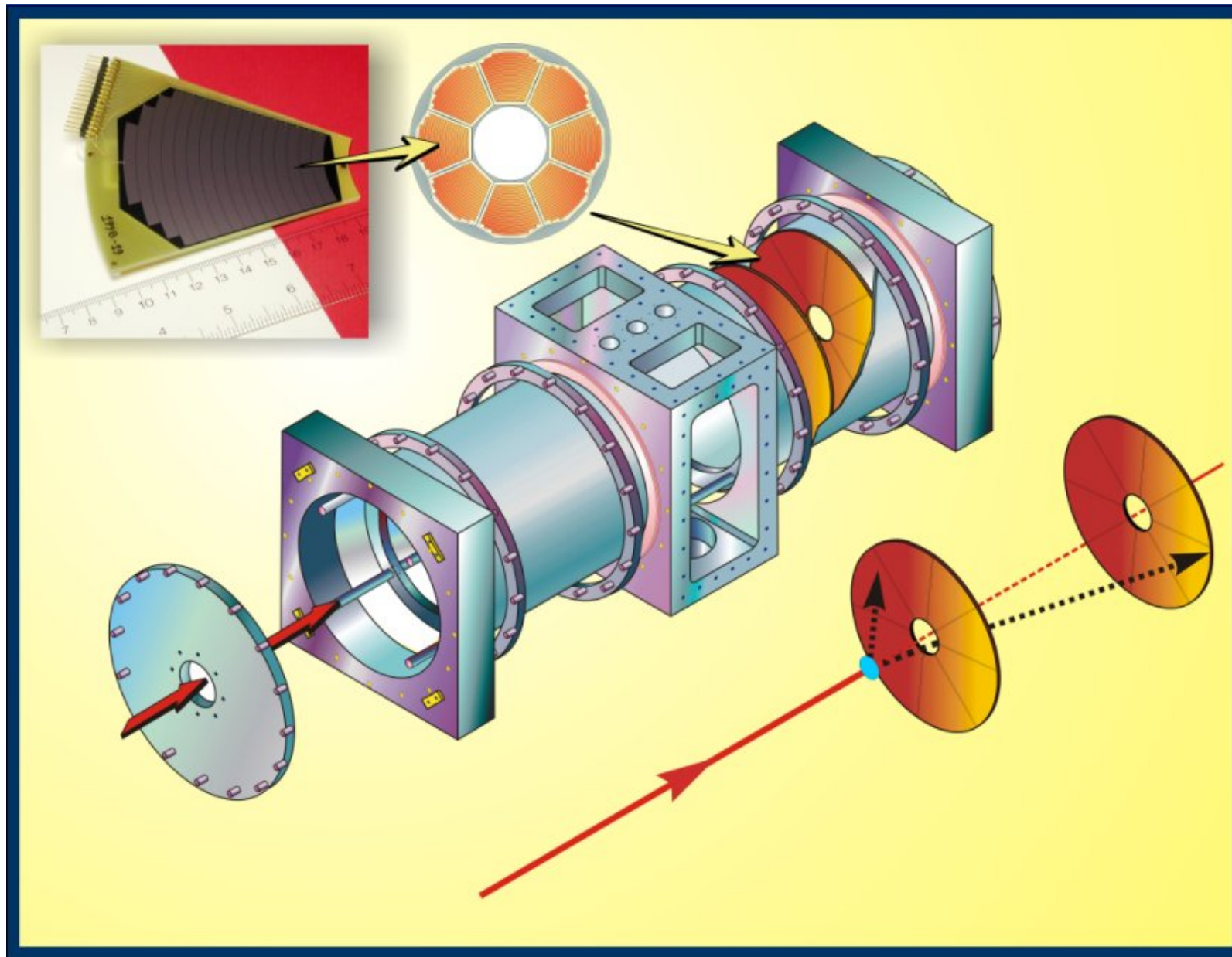
Particle ID spectra:

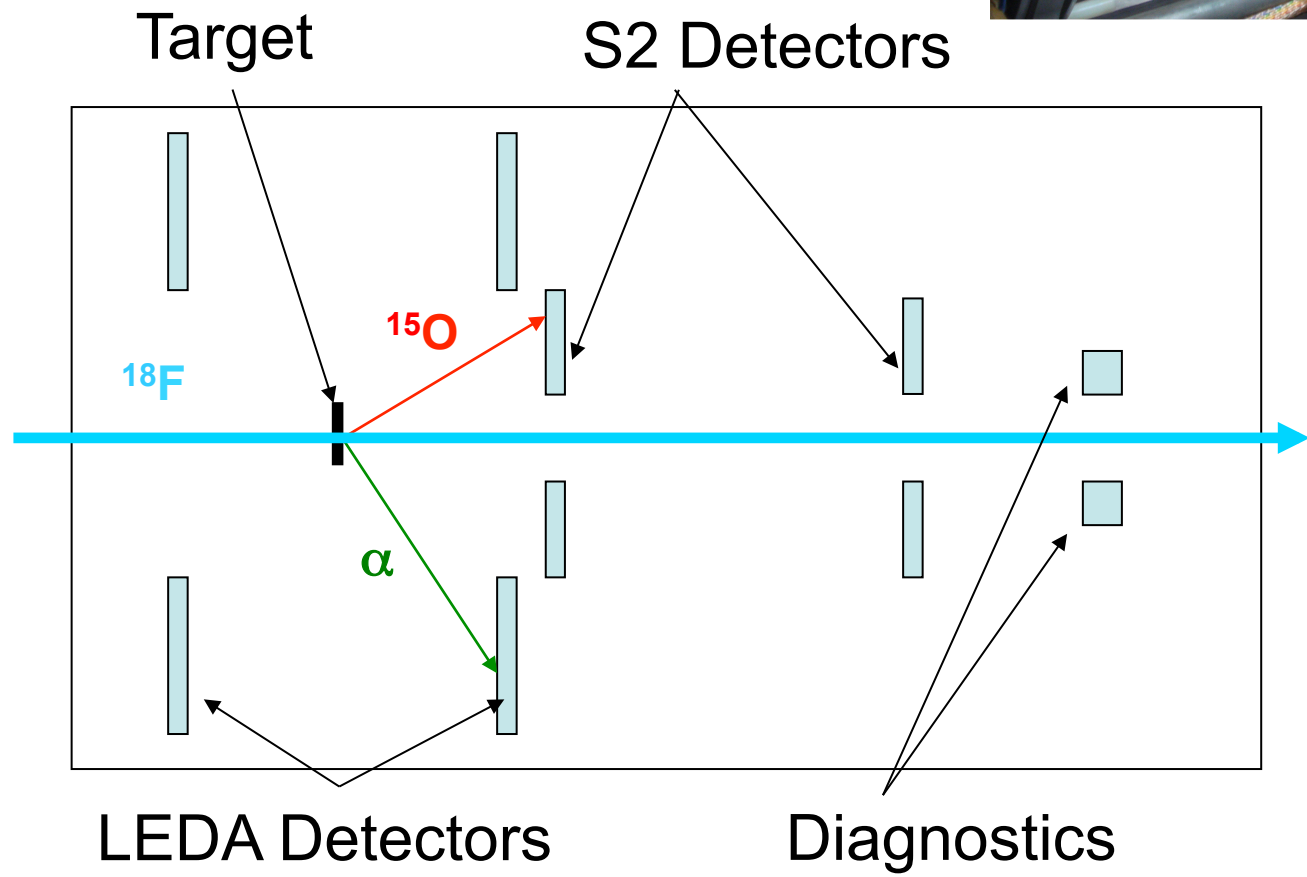
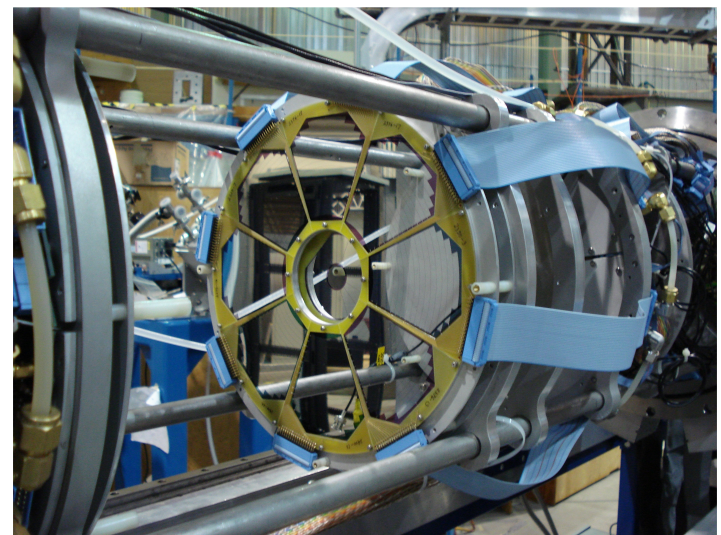


- ✧ Two good events identified in nine day run
- ✧ Resonance strength found to be ~ factor 10 lower than expected

TUDA Silicon array

TRIUMF UK DETECTOR ARRAY - TUDA

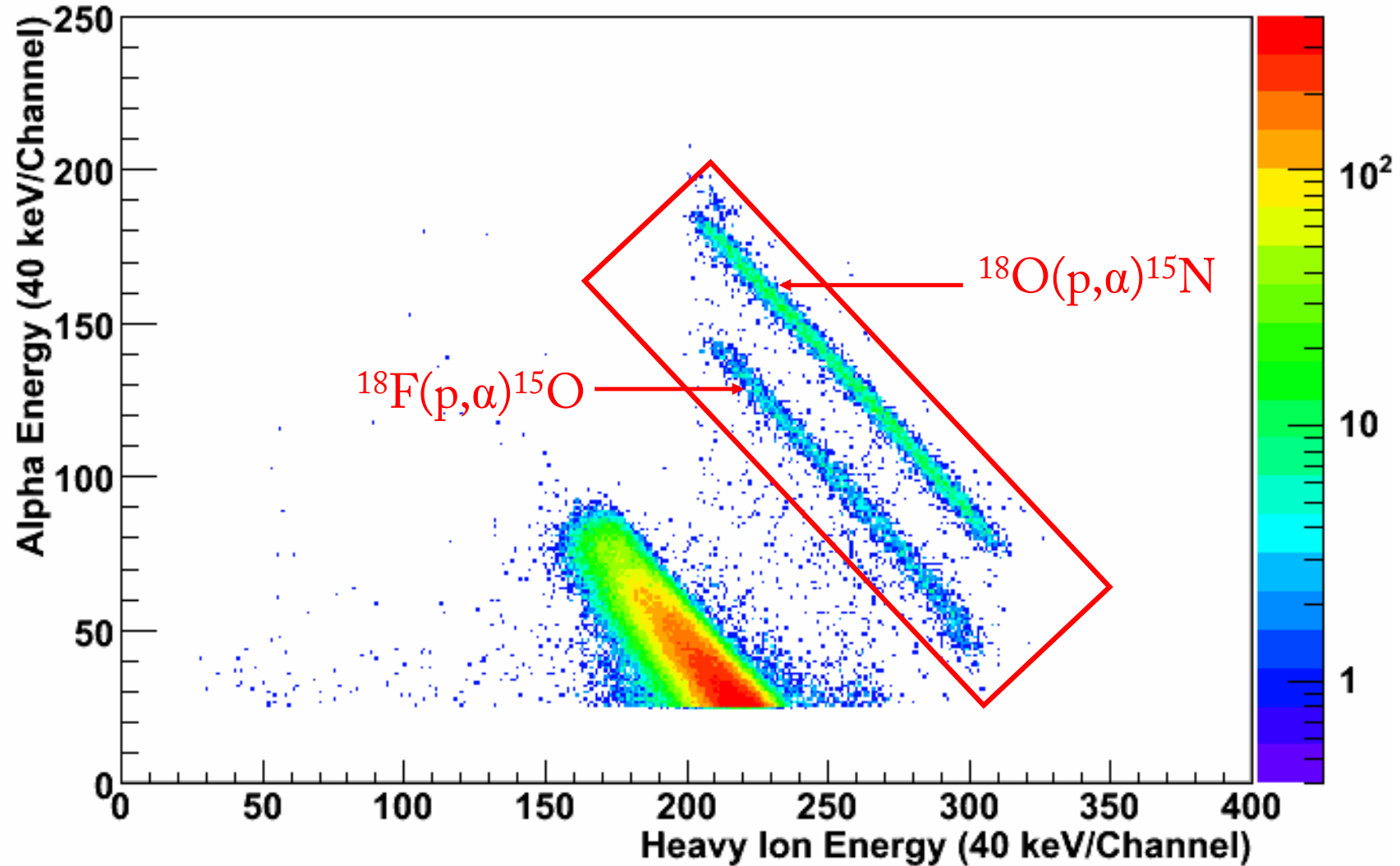






The $^{18}\text{F}(\text{p},\alpha)^{15}\text{O}$ Data

665 keV resonance





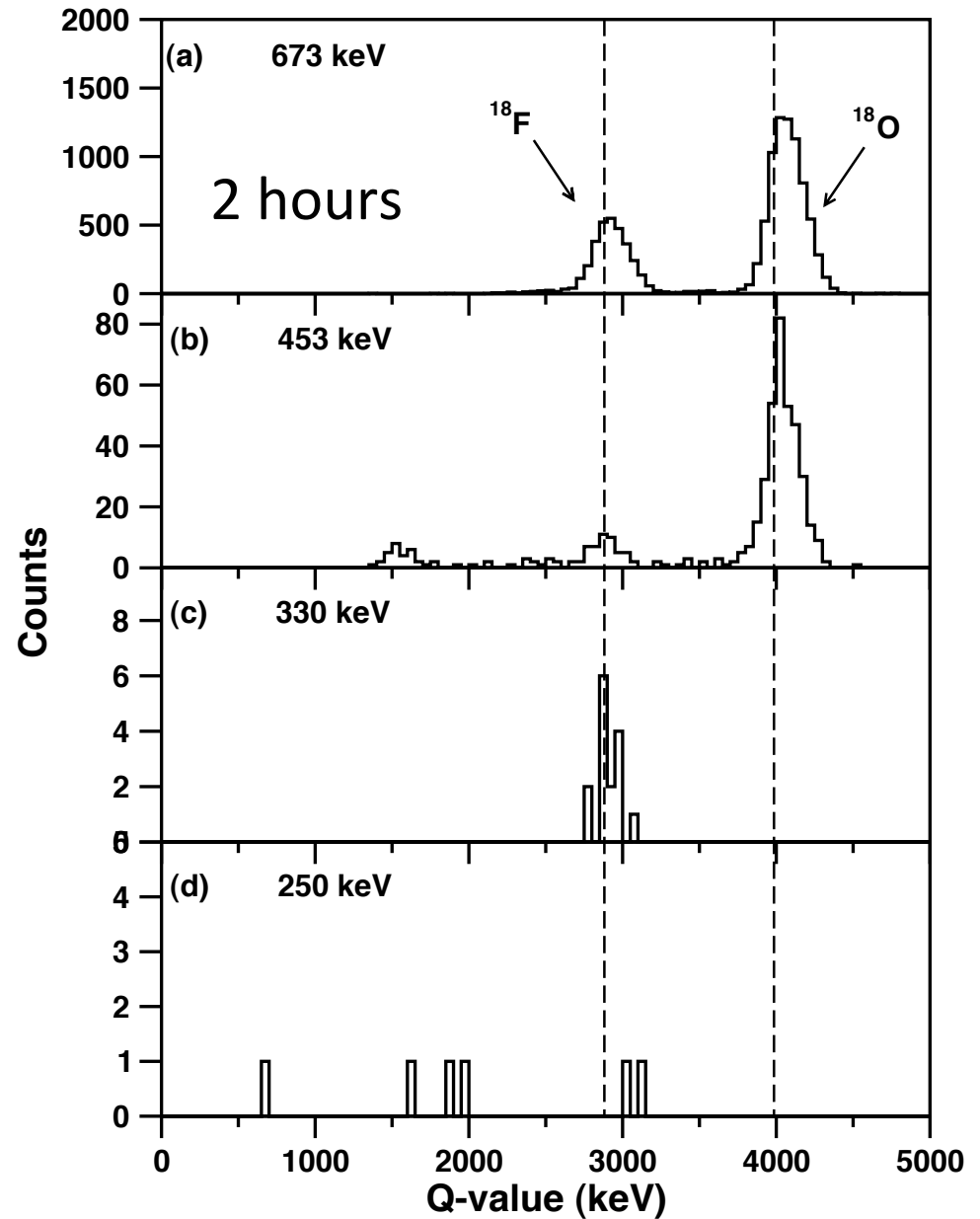
The $^{18}\text{F}(\text{p},\alpha)^{15}\text{O}$ data

- Gate on energy-energy
- Gate on ϕ correlation
- Gate on θ correlation

12 hours

15 hours

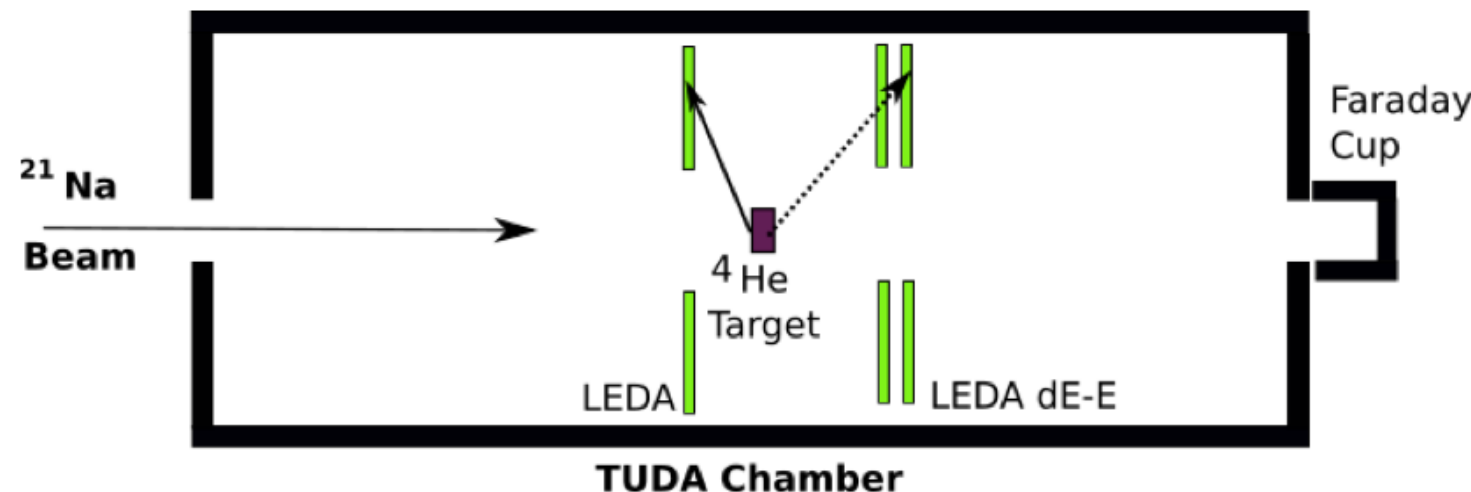
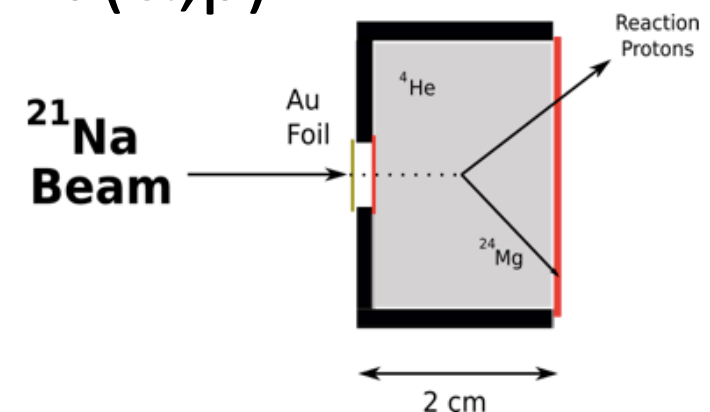
5 days



Helium target – $^{21}\text{Na}(\alpha, p)$

Standard TUDA Gas Target Experiment:

- Inverse Kinematics: ^{21}Na beam on ^4He gas target
- Reaction protons detected in LEDA telescope
- Heavy Recoil stops in Ni exit foil
- Background protons: elastics from window and fusion evaporation
∴ Gas Out runs
- Au foil provided beam (N_b) normalisation
- Elastic alphas provided $N_t \times N_b$ normalisation
- Technique previously used for $^{23}\text{Na}(\alpha, p)^{26}\text{Mg}$ - **PRL 115, 052702, July 2015**



Gas detectors

ANASEN detector – LSU

Array for Nuclear Astrophysics and Structure with Exotic Nuclei

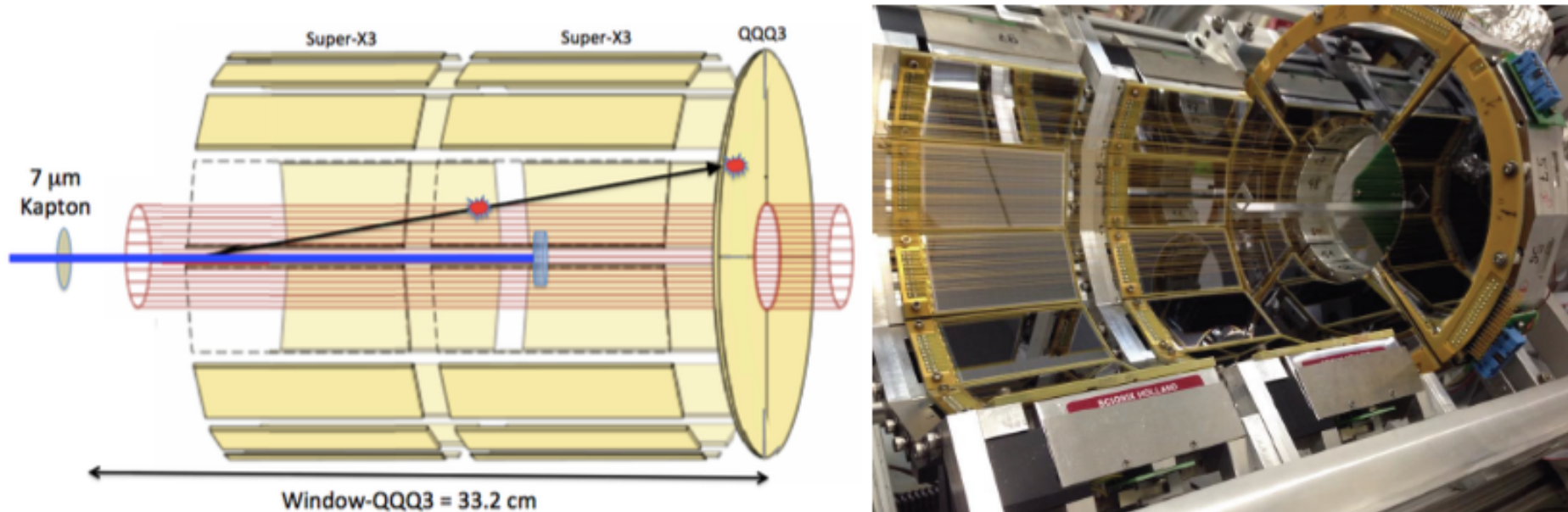


FIG. 4: (left) Cartoon of the basic ANASEN configuration. (right) Photo of ANASEN with half the outer detectors removed, showing a retractable solid target that can be inserted for calibrations or solid-target measurements.

Picture from TRIUMF proposal - J. Blackmon

MUSIC – Multi-Sampling Ionization Chamber

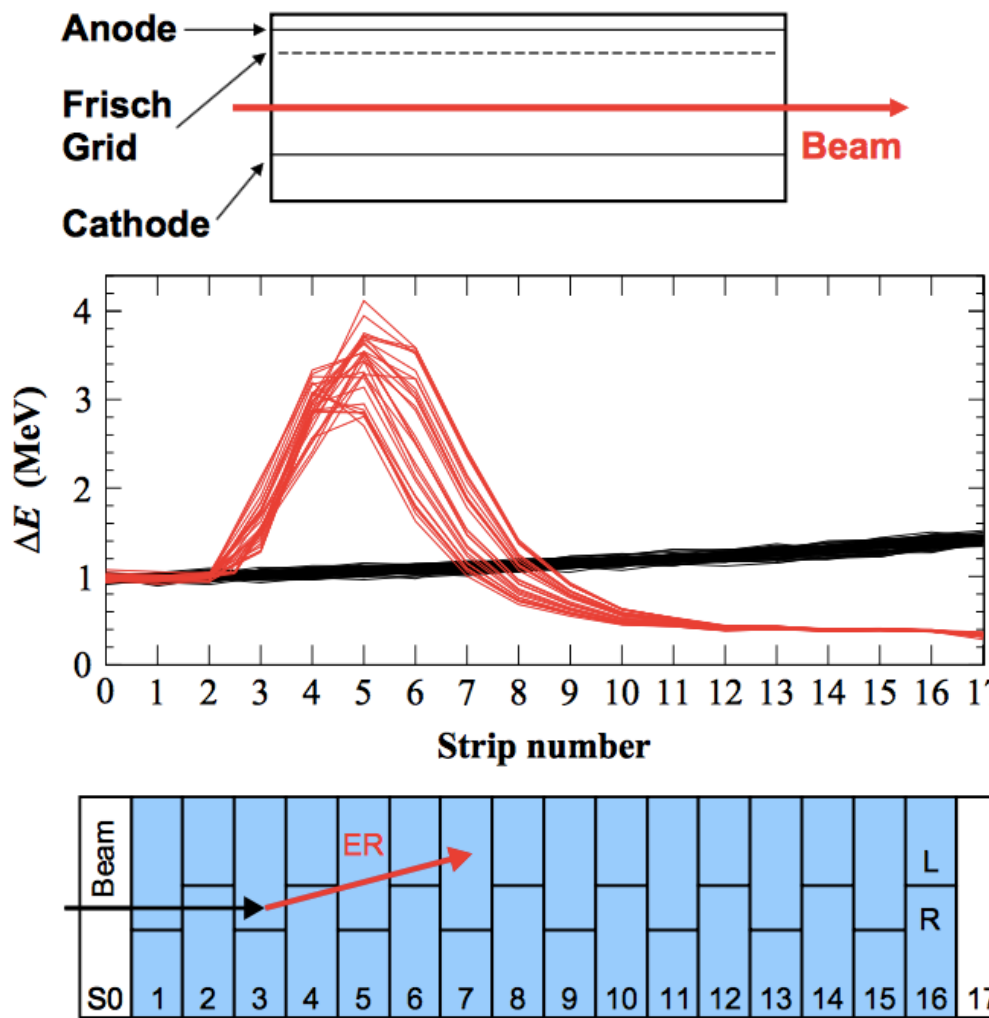


Fig. 2. Experimental traces measured with the MUSIC detector. Black lines correspond to beam particles interacting with the gas target only by ionization. The red lines correspond to fusion events occurring in strip number 3. Note the presence of the fusion features described in the text, meaning a jump in ΔE followed by zero pulse height in strips higher than 10. (For interpretation of the references to color in this figure legend, the reader is referred to the web version of this article.)

6. Indirect techniques

- ✧ Assume that the compound nucleus has no “memory” of formation
- ✧ The properties of the excited states in the compound nucleus do not depend on the population mechanism. (*Remember want to know energy, Jpi , partial and widths.*)
- ✧ The states that are populated in a given reaction depends on the structure and spin/parity of the state
- ✧ Populating reaction used depends on purpose of measurement
 - ✧ If want to determine state energies, use a reaction that is non-selective such as inelastic scattering or charge exchange
 - ✧ If want to extract partial widths, use a reaction that populates similar states to astrophysical reaction, e.g. for neutron width use (d,p), for alpha width use ($^7\text{Li},\text{t}$)
- ✧ Energy of reaction can be chosen to maximise cross section (don’t need to match energy to Gamow window)
- ✧ Broad states are very hard to observe with most indirect techniques

Coming back to $^{18}\text{F}(\text{p},\alpha)^{15}\text{O}$ as example, this reaction has been studied indirectly via:

- ❖ $^{19}\text{F}({}^3\text{He},\text{t})^{19}\text{Ne}$ – charge exchange
- ❖ $^{18}\text{F}(\text{d},\text{p})$ – neutron transfer
- ❖ $^{18}\text{F}(\text{d},\text{n})$ – proton transfer
- ❖ $^{18}\text{F}(\text{p},\text{p})$ – resonant elastic scattering
- ❖ $^{19}\text{Ne}(\text{p},\text{p}')$ – inelastic scattering
- ❖ $^{20}\text{Ne}(\text{p},\text{d})$ – neutron pickup
- ❖ $^{19}\text{F}({}^3\text{He},\text{t})^{19}\text{Ne}$ – again - *particle and gamma coincidences*

Once state information known, can calculate cross section and reaction rate.

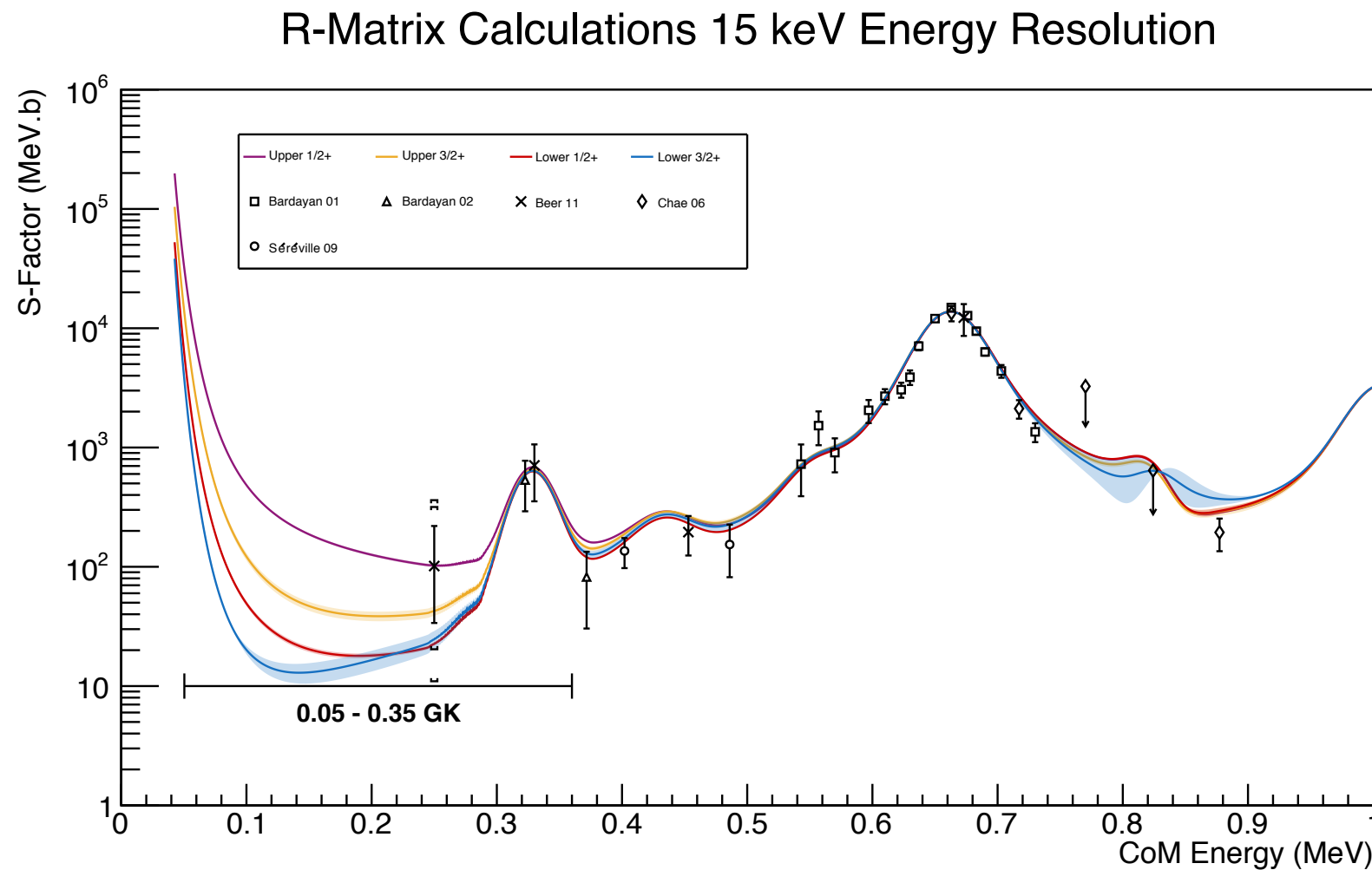


Figure from J. Riley

Conclusion

- ✧ Direct measurements preferable but often not currently feasible at relevant energies
- ✧ Indirect measurements can inform direct measurements
- ✧ Usually need combination of both direct and indirect measurements to properly constrain the reaction rate

Thank you!